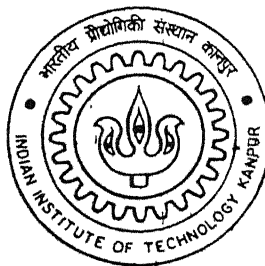# AVAILABLE TRANSFER CAPABILITY ASSESSMENT IN A RESTRUCTURED ELECTRICITY MARKET USING BIFURCATION CRITERIA

By

Sanjay Kumar Chaudhary

DEPARTMENT OF ELECTRICAL ENGINEERING
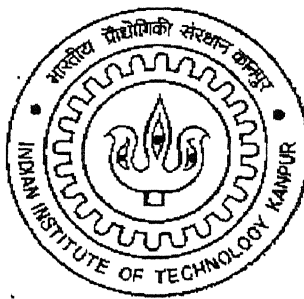## Indian Institute of Technology Kanpur
JANUARY, 2002

AVAILABLE TRANSFER CAPABILITY ASSESSMENT IN A RESTRUCTURED ELECTRICITY MARKET USING BIFURCATION CRITERIA

A Thesis Submitted

in Partial Fulfillment of the Requirements

for the Degree of

MASTER OF TECHNOLOGY

by

SANJAY KUMAR CHAUDHARY

to the

DEPARTMENT OF ELECTRICAL ENGINEERING

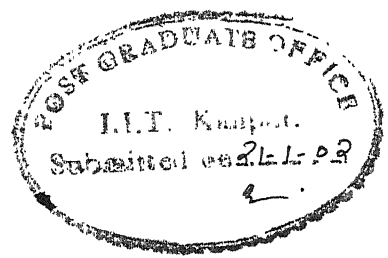# INDIAN INSTITUTE OF TECHNIOLOGY, KANPUR

JANUARY, 2002

CERTIFICATE

This is to certify that the work contained in this thesis entitled "**Available Transfer Capability Assessment in a Restructured Electricity Market Using Bifurcation Criteria**", has been carried out by Sanjay Kumar Chaudhary (Y010447) under my supervision and that this work has not been submitted elsewhere for a degree.

January, 2002

Dr. S. C. Srivastava

Professor

Department of Electrical Engineering

Indian Institute of Technology,

Kanpur – 208016

Acknowledgement

It is my proud privilege to express my deep sense of gratitude and indebtedness towards my thesis supervisor Dr. S. C. Srivastava for his excellent supervision, skilled guidance, stimulating discussions, inspiration and constant encouragement, which were the vital factors in successful completion of the present work. I am heartily thankful to him for his deep concern towards my academics and personal welfare.

I am extremely grateful to Professors Dr. S. S. Prabhu, Dr. P. K. Kalra and Dr. B. C. Pal who taught me various courses during my academic programs. I thankfully acknowledge the sincere attitude and cooperation of Dr. Sachidanand and Dr. R. K. Varma.

I am thankful to Mr. Ashwani Kumar and Mr. Barjeev Tyagi for their constant encouragement, guidance and invaluable suggestions.

I would also like to cherish the nice company of my friends Balaji, Bikash, Kishore, Manoj, Meena, Rajesh, Shankar, Saleem, Maj. Vaid, Maj. Jayesh and all the friends at the Institute for creating a pleasant atmosphere during my stay at I.I.T Kanpur. Due thanks goes to Mr. Deepak Sharma, our lab supervisor.

Last but not the least, I would like to thank the Almighty and my family members who enabled me to reach at this stage, where I could undertake the work of this magnitude.

Sanjay Kumar Chaudhary

CONTENTS

List of Figures

List of Tables

ABSTRACT

In a restructured electricity environment, the market entities need to know the power transfer capabilities of the transmission network before committing any contract. Available transfer capability (ATC) is a measure of the unutilized transfer capability in the transmission network available for further commercial transaction over and above already committed uses. The present work proposes the application of bifurcation criteria for ATC determination. Hopf bifurcation limit has been considered for determination of the dynamic ATC and saddle node bifurcation limit for the static ATC. The proposed method is applied for various bilateral transactions on 9-bus WSCC and 39-bus New England systems. The results of ATC computed using the bifurcation criteria and bus voltage limits are compared for different transactions under two different scenario of load increase and for constant power as well as voltage dependent load models.

Available transfer capability can be enhanced using FACTS controllers. In the present work, the use of SVC, which is one of the popular FACTS controller already installed by many utilities has been studied for the enhancement of the system power transfer capabilities. A method based on the eigenvalue analysis and the bus voltage states corresponding to the critical mode has been utilized to decide the optimal placement of SVC. ATC values have been computed using the bifurcation criteria and the bus voltage limits for the different transactions in the two test systems with the optimal placement of SVC and compared with those obtained without SVC in the system.

CHAPTER 1

INTRODUCTION

1.1 General

Over the last century, electric power system has evolved as large integrated system throughout the world. Electric energy is the most common and convenient form of energy. In earlier days, state-owned vertical monopolistic electric utilities were essential for development, expansion and standardization of the electric power industry. Now these goals have been achieved and the industry has matured enough to drive itself.

The existing rules of monopolistic market authorize a single utility to generate, transfer, distribute and sell electricity in a region, state or a country. Utilities have to operate according to the government policies, guidelines and regulations; and are assured of fair returns without bearing any risk. This breeds incompetence and lethargic attitude in the industry as they lack the motivation. In order to dispense with the inefficiency, incompetence and other adversities of the monopolistic market, most of the utilities throughout the world are undergoing restructuring.

Restructuring of the power industry, also known as deregulation, aims at abolishing the monopoly in the generation and trading sectors thereby introducing competition at the wholesale as well as retail levels. Private entities can participate in the generation and distribution or trading sectors. Several independent power producers are expected to generate electricity. Such generating companies (Gencos) may thereafter enter into bilateral or multilateral contracts to supply the generated power to the power dealers or bulk consumers/distributors in a contractual manner or sell the power in a power-pool in which the power dealers/customers also participate in meeting their demand. In a power-exchange, the buyers can bid for their demands along with their willingness to pay. Power generation and trading will, thus, become free from the conventional regulations and be competitive. Restructuring is expected to draw private investment, increase efficiency, promote technical growth and improve customer satisfaction as different parties compete with each other to win their market share and remain in business.

1.2 Deregulated Power Market:

According to Phillipson and Willis [1], *"Deregulation is a restructuring of the rules and economic incentives that governing authority sets up to control and drive the electric power industry."*

Involving private players in the electric industry and subsequent introduction of competitive electricity market is the fundamental objective behind deregulation. This requires that all the parties involved in electricity business get fair and equal opportunity to execute their business plans. Open access is the key to a free market. In electric industry only the generation and trading is made accessible to private players. A single interconnected transmission system is a necessary monopoly so as to avoid the duplicity and to take the advantage of the interconnected network viz. reduced installed capacity, increased system reliability and improved system performance. This, in fact, benefits the electricity market.

Power producers (sellers) and dealers/customers (buyers) have to share a common transmission network for wheeling the generated power from the point of generation to the point of consumption. However, since power cannot be stored in significant amount with existing technologies, power industry differs from other industries. The balance between the electricity generation and demand plus losses has to be maintained all the time. Any imbalance in power supply and demand will lead to instability of the whole interconnected system. Further, unlike the transport network for commodities, the power flow over different available paths in the network remains uncontrolled to a large extent. Basically, it depends upon physical laws based on path admittances. Even with modern power-electronic based Flexible AC transmission system (FACTS) controllers, under load tap-changers (ULTCs) and phase-shifters, there is little control over the path taken by electric power injected at one node and drawn at the other node in the network.
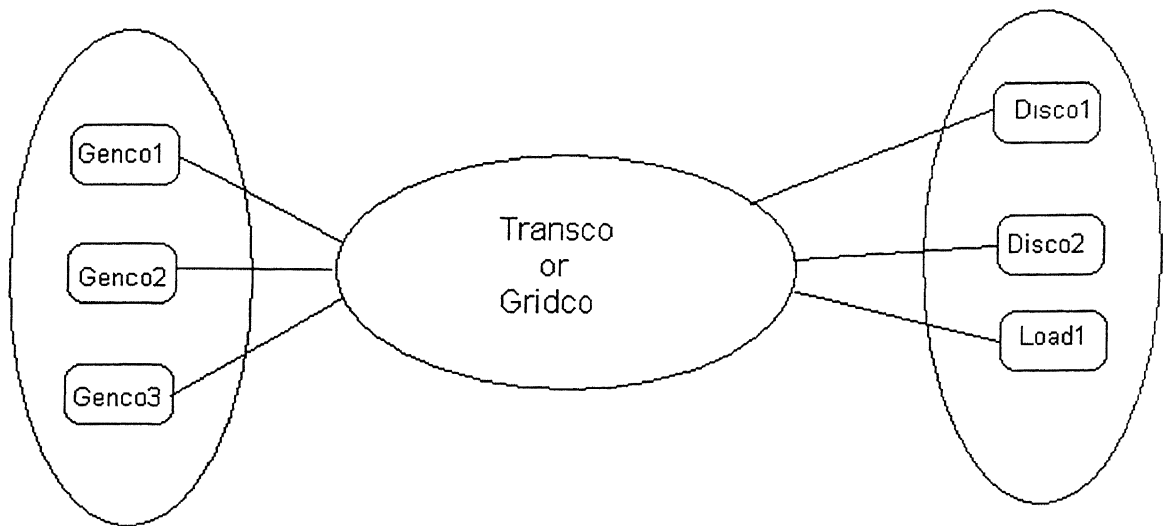
Fig. 1.1 Deregulated Power Market Structure

In the prevailing structure of an integrated power industry, a single utility is involved in generation, transmission and distribution. There may be a separate utility for each of these three tasks but in a region only one such utility is allowed for each task. The generators are therefore optimally scheduled to minimize the cost of generation, to incur minimum transmission and distribution losses, while ensuring the security and reliability of the system. Generation, transmission and distribution behave as a single entity and there is no competition at all. In a deregulated scenario, however, the activities of all different parties involved in generation and distribution together decide the generation schedule and load dispatch. The behaviour of Gencos and Discos are guided by their own commercial and organizational objectives. Consequently the power flow pattern in a deregulated environment is very likely to be different from those in existing regulated ones. All parties will try to reap the benefits of cheaper source and greater profit margins leading to overloading and congestion of certain corridors. This may well exceed the thermal, voltage and stability limits thereby undermining the system security. Further some players may try to exercise unduly larger command over the market by exploiting the system limitations.

Thus, there is a need of a regulatory body to manage the transmission network, its operation, security and reliability while ensuring its open access to all the market entities. The Independent System Operator (ISO) or the Grid Operator (Gridco) is envisaged as a regulatory body with the objectives to look after the network system and to provide open and fair access to all the market participants. Since the transmission system is shared by all the market entities, they need to know about the status of the system and the transfer capability available in the system for further commercial transactions. All power transfer contracts have to be within the bounds of the available transfer capability of the system. In some cases the market players have to reserve the transmission capability for their contract obligations. Such reservations can be allowed only within the system limits.

1.3 Role and Importance of ATC

Available Transfer Capability (ATC) indicates the unutilized transfer capacity of the transmission network that is available for reservation by the market entities. Power transaction between a specific seller bus/area and a buyer bus/area can be committed only when sufficient ATC is available for that interface and then the power companies may reserve the transfer rights as per their needs. Thus, any commercial transaction is restricted by the ATC so as to ensure the system security. Hence, the information about the ATC is to be continuously updated and made available to the market entities through the Internet-based Open Access Same time Information System (OASIS). Concerned parties check the ATC posted on the OASIS before they proceed with any transaction otherwise the transaction may have to face curtailment.

In a deregulated market, the importance of ATC can be listed as follows :

- The value of ATC reflects the amount of power transfer that can be permitted between the specified interfaces. Private parties enter into contract on the basis of ATC posted on OASIS.

- Since power transfer limits, contingency constraints, voltage limits, static and dynamic limits are taken into account while calculating the ATC, the system security is ensured as long as new power transfers are within the ATC limits.

- Private parties get an idea of the unused capacity of the system. This helps in forming their bidding strategy and market participation policies. The market entities get information in advance, if there is congestion in any part of the system by the low value of ATC posted.

- When information about both recallable and non-recallable ATC (subsequently defined in chapter-2) is available, market entities can go for firm and non-firm transmission reservation as per their needs and the available ATC in respective cases.

- The ISO has to restrict all transactions within ATC limits. In case of congestion, it can help relieve the congestion as it has the knowledge of the limiting constraint.

- In the planning horizon, the ISO or the Gridco gets information about the low value of ATC in some crowded corridors. It can plan to increase the ATC along the busy corridors and thus enhance market competition. Laying down of new lines, installation of compensators, FACTS devices and phase regulators can be planned to increase the ATC in congested corridors.

- Wheeling charges may be decided on the basis of ATC figures so as to reduce the congestion. Higher the ATC, lower may be the wheeling charges and vice-versa. This measure would partly help to relieve the congestion.

1.4 State-of-the-Art

In the last few decades, there has been tremendous increase in both the generation and demand of electric power. However, power transmission lines have not increased proportionately. Therefore, even before deregulation, the need to maximize the utilization of existing transmission network was realized. It is a cost effective and technically viable alternative to laying down new lines. Rising cost of right-of-way (ROW) and general opposition to new overhead lines are the main impediments for new lines. The solution lies in maximizing the use of existing ones. All this has led to the overloading of transmission lines. Usually, for High Voltage and Extra High Voltage lines, thermal limit is not the limiting constraint, but voltage and stability limits are the limiting constraints. There are several

instances of Voltage collapse due to system overloading [7] – New York Power Pool disturbances of September 22,1970 and Swedish System disturbances of December 27,1983 are to name a few.

NERC [9] defined terms like First Contingency Total Transfer Capability (FCTTC) and First Contingency Incremental Transfer Capability (FCITC). The terms TTC and ATC, as defined in context of the deregulated market, are more or less similar to these terms respectively except that the latter are dependent on the interface considered for a specific transaction. Previously, there used to be a single system and hence there was no concept of specific interfaces.

Deregulation of the electric power market is a challenge in itself [1,3]. Research work worldwide is focused upon the technical and computational requirements and feasibility studies for the new market structure. Study of the market feasibility and the associated methods are an important research area these days.

ATC is the amount of additional power that can be transferred from source bus/area to the sink bus/area. One simple approach would be to consider a suitable base case for the specified time period and repeatedly increase the system loading and generation simultaneously as long as the load-flow algorithm converges and none of the limits are violated. The loading and generation schedule should be as per the transaction considered. Continuation Power Flow [29] uses tangential predictor and subsequent corrector algorithm to give the load-flow solution over the entire range of possible voltages. Ejebe et al [24] suggested the use of this algorithm for ATC determination. Source and sink busses were identified and using distribution factors the loading and the generation was increased simultaneously so as to reflect the transaction under study. The maximum increased amount of loading, for which all the limits viz. line-flow, voltage and contingency were satisfied, was the ATC for the given transaction at the specified base conditions.

Full ac power-flow schemes are bound to be computation intensive and so the use of dc load-flow method and linearity based schemes have been suggested [15,20]. In ref [20],

power transfer distribution factors (PTDF) are derived from the system reactance matrix. These are constant for a given system and any change depends on the line contingency. The margin between the thermal limit of the line and the base case flow on it is divided by the PTDF corresponding to the transaction considered. This gives the maximum value of the transacted power and thus the ATC. In [15], the topological information of the system is stored in matrix form and, therefore, the constants for different simultaneous cases and critical contingencies can be calculated beforehand and used for calculating the ATC value. The method can handle simultaneous transfers and contingency cases. Since the PTDFs are constant and are determined beforehand and the process is linear, the system is extremely fast. However, only thermal limits can be considered as voltage and other stability limits cannot be satisfactorily represented in terms of the line power flow limits. Moreover, the system does not provide any idea about the system losses, reactive power requirement and bus voltage profile at the maximum loading. Hamoud [16] proposed an optimization-based method using DC load-flow. A large fictitious load and a large fictitious generator with very high cost-function were assumed to be attached to the buyer bus and a large but cheap generator to the seller bus. The generation at the seller bus was to be maximized through optimization. Though the approaches in [15, 20] seem to be different, basically they are the same.

In Refs. [11,23] sensitivity indices derived from ac load-flow Jacobian and linearized system equations are used. In [11], localized linearity of the system is assumed and the additional loading required to hit the different transfer limits are separately calculated and the minimum of all these is taken as ATC. With system loading and generation increased corresponding to this ATC value, an AC load-flow is run. The process is iterated till the change in maximum loading becomes insignificant and thus maximum loading point is obtained. The base case can be subtracted from this TTC to get the value of ATC. A similar method is described in [23]. The limiting constraint is identified in each iteration and then it is used as the only constraint in the succeeding constrained power-flow steps to get the precise solution at the maximum loading point.

The method described in ref [22], first determines the maximum transfer capability subject to line thermal limits and DC load-flow routine. Then the value of ATC obtained so

is refined using AC load-flow and voltage as well as reactive power limits. Shabaan [19] proposes floating point based Genetic Algorithm to calculate the TTC value and hence estimate the ATC value. The objective function used here is to maximize a point-to-point power transaction without violating the system constraints.

Most of the works are thus concerned with static limits such as thermal, voltage and reactive power generation limits. Certain parts of the transmission network are likely to be operating under stressed conditions. The system may be stable on the basis of static criteria but it may experience oscillations leading to instability when some disturbance occurs in the system. Hisken et al [26] developed a minimization-based iterative approach for computing dynamic ATC. Time functions of both continuous and discrete dynamic states and algebraic variables were used and solved to find the unstable equilibrium manifold. The distance between the base case operating point and the manifold gives the value of ATC. Tuglie et al [18] linearized the post-fault transient swing equations and solved them at small discrete intervals. While maximizing the power transaction along the desired interface, dynamic constraints were used for these equations to check that the system returns to a stable equilibrium point after the removal of the fault.

Bifurcation analysis [10,17,21,27] has been applied in the study of the voltage stability. Saddle node bifurcation is associated with steady state voltage collapse while the Hopf bifurcation indicates the oscillatory instability. At Hopf bifurcation [10], a system, which was previously in stable equilibrium begins a steady state oscillation in a periodic orbit (supercritical Hopf bifurcation) or with a growing oscillatory instability as a parameter is slowly varied (subcritical Hopf bifurcation). The restructured market, too, may face voltage instability problems. However, in the literature surveyed, the bifurcation analysis has not been applied in the assessment of ATC.

Since ATC is the measure of the transfer capability of the system above the operating base case. Any technique, which increases the transfer capability of the system, naturally increases the ATC values of the system. Series and shunt compensations are long known for their ability to enhance the system power transfer capability as well the stability. FACTS

controllers are power-electronic based compensating devices and may be used to increase the ATC as well as the dynamic stability. Ref [14] suggests the placement of TCSC and TCPAR on the basis of improvement in a performance index defined as the fractional change in power transfer after the device is installed in the concerned line or at the concerned bus Static model of these devices have been considered and the TTC is assessed by repeated load-flow with increasing loading and generation simultaneously. Cañizares [25] proposed the second order sensitivity analysis for determining the optimum placement of SVC and TCSC. Gupta [17] suggested the eigen-value analysis of the complete system Jacobian and study of the participation factors corresponding to the critical eigen-value to determine the load-bus most suitable for placing the SVC.

1.5 Motivation:

Limited literature survey presented in the earlier section reveals that most of the work on ATC considers only the static limits as the system constraints. Power system network is a complex interconnection of a large number of machines and loads through transmission lines. With continuously varying generation schedule and loads it is always in quasi-static state. The generator, turbine and field excitation system exhibit a dynamic response under disturbances. The dynamics of the system as a whole, when subjected to small and large disturbances, has to be studied and analyzed for stability. These studies come under the purview of dynamic stability and the ATC calculated considering the dynamic stability limits is therefore known as dynamic ATC.

Bifurcation analysis has been applied in Voltage Stability studies [5,6,7,17,27]. Hopf bifurcation is associated with dynamic voltage instability while Saddle Node bifurcation is concerned with the steady state (static) voltage stability limit. However, bifurcation approach has not been applied in ATC calculation. Apart from considering the static limits, application of bifurcation analysis would be a novel idea in the assessment of dynamic ATC.

Reactive power flow over the transmission lines poses another limit on stability. Load compensation and additional reactive power support is expected to improve the total transfer

capability of the system and thus enhance the ATC. FACTS based compensating devices like TSC, SVC, TCSC, UPFC etc. will provide reactive power compensation to the system thereby improving the ATC of the system as well as the system stability due to their better controllability.

Hence, the main objectives behind the present work have been the following :

- To evolve a procedure for ATC determination utilizing bifurcation concept.

- To compute both static and dynamic static considering saddle node bifurcation (SNB) and Hopf bifurcation (HB) limits respectively.

- To study the impact of FATS controllers (only SVC considered in the present work) on important improvement of static and dynamic ATC.

1.6 Thesis Organization:

Chapter-1 introduces the general concepts of deregulation of electricity market. The need and importance of ATC in the new market structure is briefly discussed and the motivation behind the present work has been brought out.

Chapter-2 first presents a detailed description of ATC and defines the associated terms. A method has been proposed to compute static and dynamic ATC considering Hopf bifurcation (HB), saddle node bifurcation (SNB) and bus voltage limits.

In chapter-3 a criterion for optimal placement of SVC is given. The impact of including SVC in the system has been studied after incorporating the dynamic model of SVC in WSCC 9-bus and New England 39-bus systems.

Finally chapter 4 concludes the main findings of the research work carried out in the thesis and brings out few areas of further research in the determination of ATC values and its enhancement.

CHAPTER 2

ASSESSMENT OF AVAILABLE TRANSFER CAPABILITY

2.1 Introduction

The operating state of a transmission network is characterized by the generation scheduling and load dispatch, status of circuit breakers, reactive power support at different nodes in the system and tie line flows. In real time application, these parameters are estimated with reasonable accuracy through data acquisition and state estimation software. Data for future operating states can be predicted using load forecasting and generation scheduling techniques. A well-built transmission system generally possesses the capability to transfer power over and above the base case transfer. The transmission company (Transco) or the Grid operator (Gridco), in a deregulated market, has to evaluate the amount of extra power that can be allowed along different corridors and inform the market of its availability, so that they can reserve the same. Available Transfer Capability (ATC) is a measure of the unutilized capacity of the transmission network that can be traded in the power market.

DC load-flow and PTDFs have been used in references [15,16,20] for fast but approximate determination of ATC. Sensitivity based methods have been reported in references [11,22,23]. All these methods have considered static limits viz. line-flow/thermal limits, bus voltage limits, reactive power generation limits etc as the constraints. References [18,26] incorporate the transient dynamic equations for calculation of dynamic ATC. Bifurcation analysis [4,6,10,21,27] has been applied for voltage stability studies. Hopf bifurcation is a good indicator of dynamic voltage instability while saddle node bifurcation gives the static voltage stability limit. These concepts have, however, not been applied to the ATC calculation. This chapter has explored the application of bifurcation theory for the determination of dynamic and static ATC values. The proposed method has been used for TTC and ATC calculation on 9-bus WSCC System and 39-bus New England System based on Hopf bifurcation, saddle node bifurcation and voltage limit constraints.

CHAPTER 2

ASSESSMENT OF AVAILABLE TRANSFER CAPABILITY

2.1 Introduction

The operating state of a transmission network is characterized by the generation scheduling and load dispatch, status of circuit breakers, reactive power support at different nodes in the system and tie line flows. In real time application, these parameters are estimated with reasonable accuracy through data acquisition and state estimation software. Data for future operating states can be predicted using load forecasting and generation scheduling techniques. A well-built transmission system generally possesses the capability to transfer power over and above the base case transfer. The transmission company (Transco) or the Grid operator (Gridco), in a deregulated market, has to evaluate the amount of extra power that can be allowed along different corridors and inform the market of its availability, so that they can reserve the same. Available Transfer Capability (ATC) is a measure of the unutilized capacity of the transmission network that can be traded in the power market.

DC load-flow and PTDFs have been used in references [15,16,20] for fast but approximate determination of ATC. Sensitivity based methods have been reported in references [11,22,23]. All these methods have considered static limits viz. line-flow/thermal limits, bus voltage limits, reactive power generation limits etc as the constraints. References [18,26] incorporate the transient dynamic equations for calculation of dynamic ATC. Bifurcation analysis [4,6,10,21,27] has been applied for voltage stability studies. Hopf bifurcation is a good indicator of dynamic voltage instability while saddle node bifurcation gives the static voltage stability limit. These concepts have, however, not been applied to the ATC calculation. This chapter has explored the application of bifurcation theory for the determination of dynamic and static ATC values. The proposed method has been used for TTC and ATC calculation on 9-bus WSCC System and 39-bus New England System based on Hopf bifurcation, saddle node bifurcation and voltage limit constraints.

2.2 Available Transfer Capability (ATC)

According to NERC Report [9] – *'Available Transfer Capability (ATC) is a measure of the transfer capability remaining in the physical transmission network for further commercial activity over and above already committed uses.'* The term capability here refers to the ability of the line(s) to reliably transfer power from one bus/area to another. It is different from the transfer capacity in the sense that capacity implies the rating of the specified line(s) and that accounts for the thermal limits only. Capability on the other hand is a function of the physical relationship of that line with other elements in the transmission network.

Mathematically, ATC is defined as,

$$ATC = TTC - TRM - \{ETC + CBM\}.$$
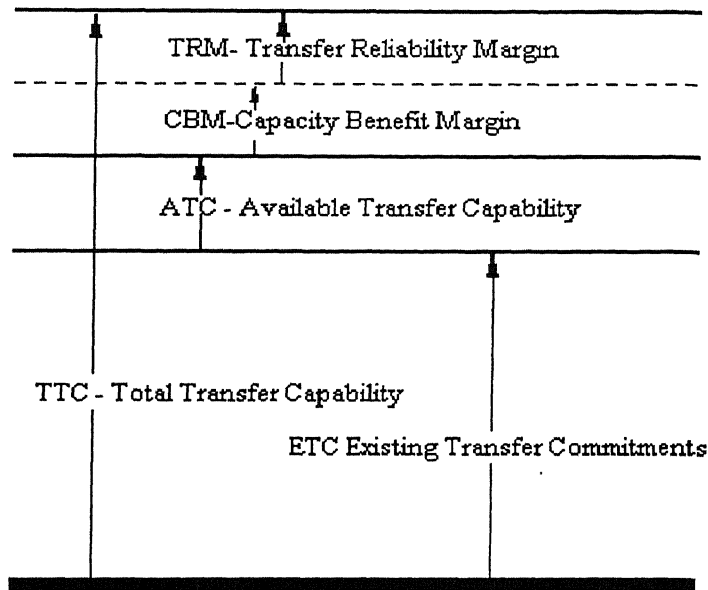
Fig 2.1 Basic Definition of ATC

The ATC between two specific areas/buses gives the upper limit of additional power flow between them for the specified time period under given conditions. Some terms associated with the definition of ATC, as shown in Fig. 2.1, are defined in NERC Report [9] are described below :

Total Transfer Capability (TTC): It is the amount of electric power that can be transferred over the interconnected transmission network in a reliable manner under a

12

reasonable range of uncertainties and contingencies. It is more or less similar to the First Contingency Total Transfer Capacity (FCTTC). While determining TTC, system conditions, critical contingencies, system limits, parallel path flows and effects of non-simultaneous and simultaneous transfers are to be considered.

Transmission Reliability Margin (TRM): It is defined as the amount of transmission transfer capability necessary to ensure that the interconnected network is secure under a reasonable range of uncertainties in the system conditions.

Capacity Benefit Margin (CBM): It is the amount of transmission transfer capability reserved by the load serving entities to ensure access to generation from interconnected systems to meet generation reliability requirements. It also helps to reduce the installed capacity of the plant.

Existing Transfer Commitments (ETC) refers to the power transfer capability that must be reserved for already committed transactions.

Considering firm and non-firm transmission contracts, a particular load may be curtailed or recalled under specific conditions. ATC definition is further elaborated for such transactions using the terms curtailability and recallability.

Curtailability is the right of the transmission service provider to interrupt all or part of the transmission service due to constraints that reduce the capability of the transmission system. Curtailment of loads occurs only when the system reliability is threatened or emergency conditions exist. On the other hand, **recallability** is the right of a transmission service provider to interrupt all or part of the service for any reason, including economic, in consistence with the tariff and contract provisions and prevalent policy.

Based on the recallability concept two commercial applications of ATC are defined as follows :

Non-recallable Available Transfer Capability (NATC):

NATC = TTC – TRM - {Non-recallable reserved transmission service + CBM }

Recallable Available Transfer Capability (RATC):

RATC = TTC – TRM - {Recallable reserved transmission Service

+Non-recallable reserved transmission Service + CBM }

13

A general method of determination of ATC, TRM and CBM is given in the NERC report. However, the service provider is free to choose any appropriate method that gives the loadability of the system according to its conditions and the requirements for security and reliability. A high value of ATC will promote the commercial transaction opportunities but it will undermine the system security while a low value will unnecessarily limit the commercial transactions. Usually, TRM and CBM are decided by the utilities according to their condition and reliability requirements.

In literature describing the methods to assess the value of ATC, a simplified definition of ATC is considered. According to Gravener and Nwankpa [22], '*The ATC is the limiting transfer value between two control areas (source and sink) that is available without any violation of power system operating properties, e.g. thermal overload and voltage limits.*' It provides an indication of the amount of additional electric power that can be transferred from one area to another for a specific time frame and for a specific set of conditions.

The inclusion of TRM and CBM in the value of ATC as defined above is implied The ISO or the Transco has to set aside appropriate margins from the ATC. CBM may be traded by the generating entities to ensure their own reliability.

2.3 Principles of ATC Determination

The basic objective of the determination of ATC is to tell the market entities about the system limitations beforehand in terms of additional MW of power that can be transferred from one area to another. Since private parties are interested only in commercial aspects, it is the responsibility of the ISO to determine, update and post the current value of ATC for every time interval. Following are the governing principles for ATC determination :

1. ATC calculation must produce commercially viable results. ATCs produced by the calculations must give a reasonable and dependable indication of transfer capabilities available to the power market.

2. ATC calculations must recognize time-variant power flow conditions on the entire inter-connected transmission network.

14

3. ATC calculations must recognize the dependency of ATC on points of electric power injection, the directions of transfers across the interconnected transmission network, and the points of power extraction.

4. Regional and wide-area co-ordination is necessary to develop and post the information that reflects the ATCs of the inter-connected transmission network

5. ATC calculations must conform to NERC (or equivalent regulatory guidelines in the specific country), regional, sub-regional, power pool, and individual system reliability and operating policies, criteria or guides.

6. The determination of ATC must accommodate reasonable uncertainties in system conditions and provide operating flexibility to ensure the secure operation of the interconnected network.

2.4 Factors Affecting ATC

The existing transaction commitments (ETC) is known precisely only for the real time applications. For any other time interval in future, this has to be approximated by forecasting techniques. The ETC determines the base case operating point for the specified time interval. It includes the generation schedule, load dispatch, system configuration, state of all the circuit-breakers and contingencies, if any. The margins TRM and CBM are decided as per the relevant policies of the system operator and the market participants. In general, the ATC is defined by,

$$ATC = TTC - ETC.$$

TRM and CBM are to be accounted for separately when such definition is used for ATC determination. It shows the direct relationship between ATC and TTC. Hence all the constraints applicable to TTC are applicable to ATC and vice-versa. The limits to be considered for the calculation of the transfer capability may be broadly classified as :

1. Static Constraints:
   - Line Thermal Limits
   - Bus Voltage (magnitude) Limits
   - Saddle Node Bifurcation (Steady State Stability Limit)

2. Dynamic Constraints:

- Small Signal Stability Limit
- Large Signal Stability Limit.

2.4.1 Static Constraints

i) Thermal limits :

Thermal limits are determined by the current ratings of the line-conductors and the transformer ratings. It is the maximum amount of electric current that a transmission line, a cable and other electrical equipments, like a transformer can conduct for a specified period without getting overheated or damaged.

ii) Bus voltage limits :

The performance of most of the electric apparatus, be it the induction motors, furnaces, electronic devices or protective devices, is dependent on the supply voltage magnitude. These are designed for some nominal voltage as per its ratings. Most of the electric devices fail to operate properly at under-voltage while over-voltages stress the insulation and may be destructive. Therefore, it is common practice to limit the bus voltages within a narrow range around the normal voltage. Usually it is between $\pm$ 5% and $\pm$ 10%. As the system loading is increased the reactive power loss in the system increases and the voltages at load buses tend to fall. When loads are thrown off, the reactive power generated by the system exceeds the demand and the bus voltages tend to rise (Ferranti effect). Proper voltage control at different buses in the system requires strong and dynamic reactive power support. If the reactive power limits of the system are reached, the system voltage will sink if overloaded or it will rise if under-loaded. Both the conditions are undesirable. The ISO is obliged to supply electricity within the specified voltage range. Therefore, the voltage limits are imposed for ATC calculation.

iii) Steady state stability limit :

When the generation and loadings in a power system is gradually increased such that power balance is maintained, a limit is reached at which the load-flow fails to converge This is known as the steady state stability limit of the transmission system and is the

maximum power that the transmission network can transfer in steady state. If the load admittance is further increased in an attempt to increase the load, voltage collapse may occur and the power delivered to the load will decrease. At the steady state stability limit, which is also characterized by non-convergence of the load-flow equations, one of the eigenvalues of the load-flow Jacobian becomes zero.

2.4.2 Dynamic Constraints

i) Small signal stability limit:

Power System is always operating in a quasi-steady state as there are continuous changes in load demand, generation schedule, transmission parameters etc. For a heavily loaded system, the different control loops are already strained. With modern control systems capable of providing fast response, there is possibility of getting different control loops interacting with each other and subsequent build-up of oscillations when some disturbance appears in the system. The oscillations may grow and lead to instability in case the system is poorly damped. Such a tendency to oscillatory behaviour can be studied by eigenvalue analysis. For the oscillations to die out all the eigenvalues should have negative real part and be located sufficiently far from the imaginary axis in the complex plane. If a pair of complex eigenvalues is crossing the imaginary axis, Hopf bifurcation occurs leading to the onset of oscillations.

ii) Large signal stability limit :

A system, otherwise stable, may experience violent excursions of its states following a large disturbance such as breakdown of a large generator, a contingency on a heavily loaded line etc. Large power swings are observed and the machine angles may undergo large oscillations. The inherent system synchronizing and damping torques tend to bring the machines to equilibrium state. In the absence of sufficient synchronizing torque the machines lose synchronism and lack of sufficient system damping will lead to slow decay or build up of oscillations. The problem of angle instability is more severe in heavily loaded systems.

2.5 Modelling of Power System Components

i) Transmission Lines & Transformers :

Nominal pi-model representation has been used for transmission lines in this work. A line is represented by a series lumped resistance and reactance with half-line charging shunt admittances at the two ends as shown in Fig. 2.2. The transformer with unity nominal tap-setting is simply modelled as a resistance (usually zero) and a reactance in series; shunt branch parameters are neglected as shown in Fig. 2.3. For non-unity tapping and phase-shift, appropriate models have been used.
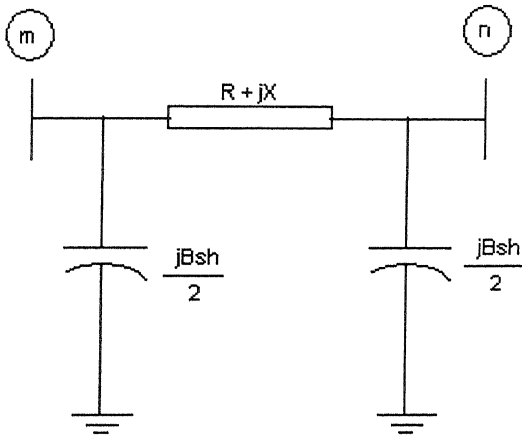
Fig 2.2 pi-model of a Transmission Line.
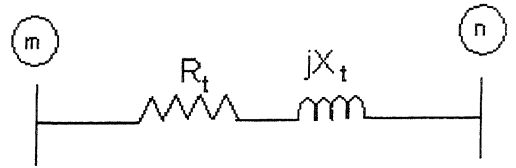
Fig 2.3 Model of a Transformer

ii) Loads :

Composite loads at various buses in steady state can be modelled as constant impedance (Z), constant current (I) or constant power (P) type. A combination of all these load models, known as ZIP-model, can be defined as given below:

$$P_{Li} = P_{CLi} + P_{Zli}V^2 + P_{Ili}V$$
$$= P_{Li}\left[a_i + b_iV^2 + c_iV\right]$$

where, P_{Li}= Total load at bus i, P_{Cli} = Constant power load,

P_{Zli}= Constant impedance load and P_{Ili}=Constant current load.

18

Constants a_i, b_i and c_i are given by -

$$a_i = \frac{P_{Cli}}{P_{Li}}, \quad b_i = \frac{P_{Zli}}{P_{Li}}, \quad c_i = \frac{P_{Ili}}{P_{Li}}.$$

ii) Generator :

Swing equations describes the mechanical dynamics of the generator. There are several models describing the field decay dynamics of the generator. In this thesis two-axis dynamic model, as shown in Fig. 2.4, has been used. The model assumes negligibly small sub-transient time constants T''_{do} and T''_{qo}. The fast dynamics associated with the damper windings are, thus, ignored. Such an approximation is justified for small-signal stability studies [4,6,7].
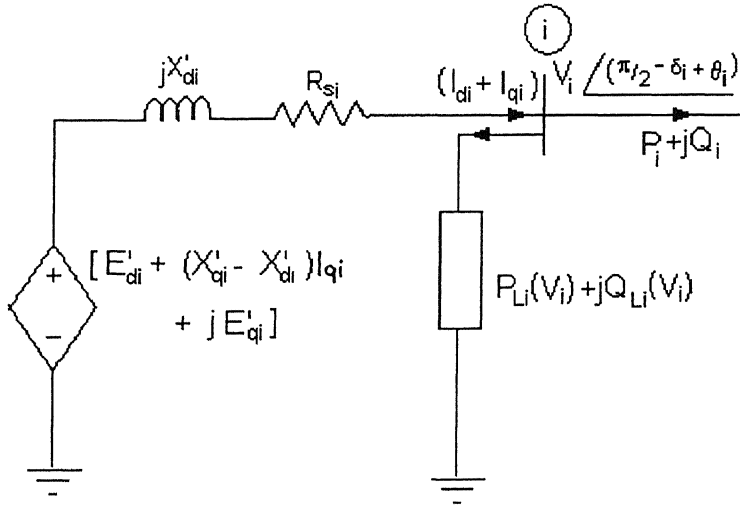
Fig 2.4 Synchronous Machine: 2-axis Dynamic Model

The dynamic equations for angle (δ_i), speed (ω_i) and stator dynamic variables E'_{qi} and E'_{di} of the i-th machine are given below :

$$\dot{\delta}_i = \omega_i - \omega_s \qquad \qquad \ldots(2.1)$$

$$M_i \dot{\omega}_i = T_{Mi} - \left[E'_{qi} - X'_{di}I_{di}\right]I_{qi} - \left[E'_{di} - X'_{qi}I_{qi}\right]I_{di} - D_i(\omega_i - \omega_s) \qquad \ldots(2.2)$$

$$T'_{doi}\dot{E}'_{qi} = -E'_{qi} - (X_{di} - X'_{di})I_{di} + E_{fdi} \qquad \ldots(2.3)$$

$$T'_{qoi}\dot{E}'_{di} = -E'_{di} + (X_{qi} - X'_{qi})I_{qi} \qquad \ldots(2.4)$$

where, δ = Machine rotor angle w.r.t. a synchronously rotating frame (in radians).

ω = Rotor speed (pu).

M = Machine inertia.

T_m = Mechanical input torque.

E'_q & E'_d = Quadrature and direct axis induced voltages behind the transient reactances.

I_q & I_d = Quadrature and direct axis stator currents.

X_q & X_d = Quadrature and direct axis stator steady state reactances.

X'_q & X'_d = Quadrature and direct axis stator transient reactances.

E_{fd} = Voltage induced due to rotor field excitation.

The subscript 'i' refers to the machine bus number.
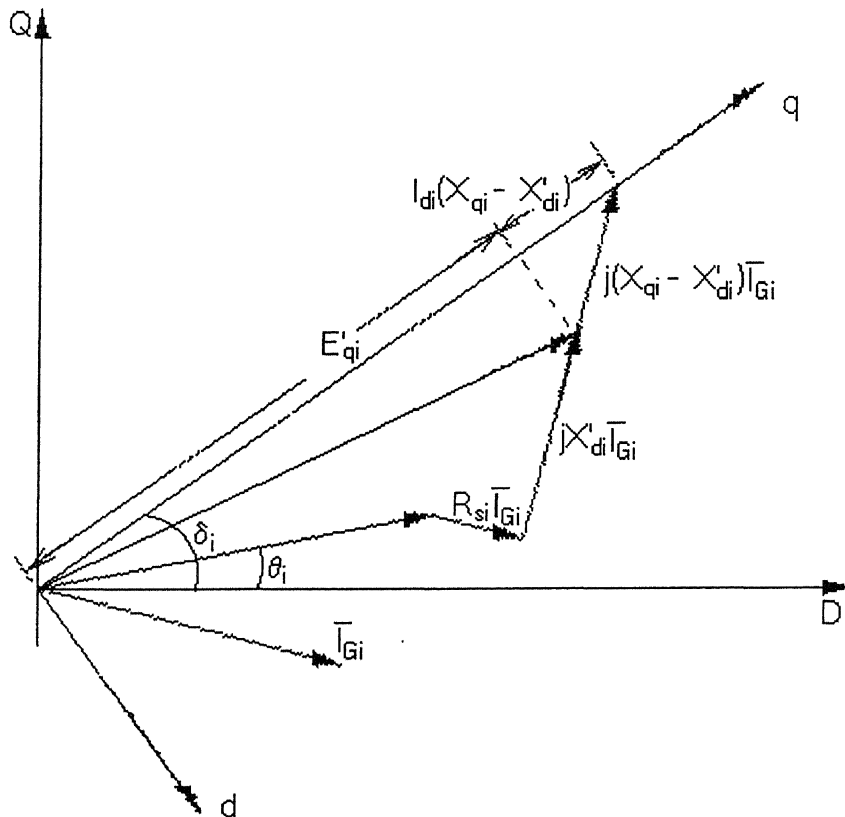
Fig 2.5 Representation of stator algebraic equations in steady state.

A vector diagram of the synchronous generator is given in Fig.2.5. The stator variables E'_{di}, E'_{qi}, I_{di}, and I_{qi} are related to the network variables – $V_i \angle \theta_i$ by the following complex algebraic equations :

$$V_i e^{J\left(\pi/2 - \delta_i + \theta_i\right)} + \left(R_{si} + jX'_{di}\right)\left(I_{di} + jI_{qi}\right) - \left[E'_{di} + \left(X'_{di} - X'_{qi}\right)I_{qi} + jE'_{qi}\right] = 0 \quad \text{.... (2.5)}$$

The power balance equation at the generator terminals is given as,

$$P_i + jQ_i = \left(V_i\right)\left(I_{di} - jI_{qi}\right)e^{J\left(\pi/2 - \delta_i + \theta_i\right)} - P_{Li}(V_i) - jQ_{Li}(V_i) \quad \text{.... (2.6)}$$

where,

$$P_i + jQ_i = \text{Real and Reactive power injected into the network at bus i}$$

$$= \sum_{k=1}^{n} V_i V_k y_{ik} e^{J(\theta_i - \theta_k - \alpha_{ik})}$$

$$\delta_1 = \text{Angle of } \left[V_i e^{J(\theta_i)} + \left(R_{si} + jX_{qi}\right)\bar{I}_{Gi}\right]$$

$$\bar{I}_{Gi} = \left(\frac{P_{Gi} - jQ_{Gi}}{V_i e^{-J(\theta_i)}}\right)$$

iv) Excitation System:

IEEE Type DC-1, DC excitation system [6] has been considered in this thesis work. It represents field controlled DC commutator exciters with continuously acting voltage regulators. The block diagram for such an exciter is given in Fig 2.6.
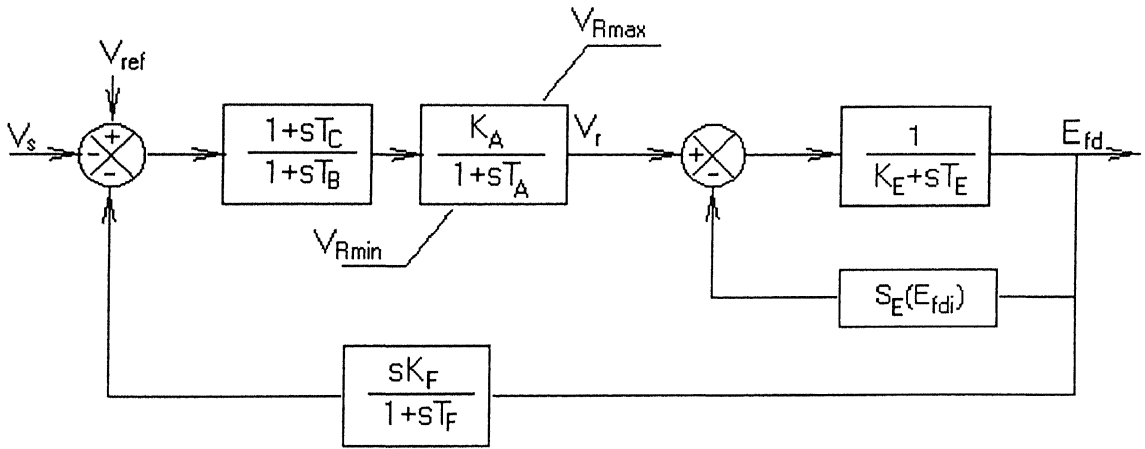
Fig. 2.6 IEEE Type DC-1, DC Commuter Exciter

The block with the transfer function $\left(\dfrac{1 + sT_C}{1 + sT_B}\right)$ represents the Transient Gain Reduction (TGR) as $T_B > T_C$ and has the function similar to that of the Excitation System Stabilizer(ESS). Normally either TGR (in forward path) or ESS (in the feedback path) is

21

used. By choosing $T_B = T_C$, the TGR is neglected. Further the limiter action has been neglected in this thesis work.

The dynamic equations for this model are :

$$T_{Ei} \frac{dE_{fdi}}{dt} = -\left(K_{Ei} + S_{Ei}\left(E_{fdi}\right)\right)E_{fdi} + V_{Ri} \qquad \ldots\ldots \text{(2.7)}$$

$$T_{Ai} \frac{dV_{Ri}}{dt} = -V_{Ri} + K_{Ai}R_{fi} - \frac{K_{Ai}K_{Fi}}{T_{Fi}} E_{fdi} + K_{Ai}\left(V_{refi} - V_i\right) \qquad \ldots\ldots \text{(2.8)}$$

$$T_{Fi} \frac{dR_{fi}}{dt} = -R_{fi} + \frac{K_{Fi}}{T_{Fi}} E_{fdi} \qquad \ldots\ldots \text{(2.9)}$$

where,

$$S_{Ei}\left(E_{fdi}\right) = A_{ex}e^{\left(B_{ex}E_{fdi}\right)} \text{ is a field saturatin function.}$$

V_{Ri} = Regulator amplfier output Voltage.

K_{Ai}, T_{Ai} = Regulator amplfier gain and time constatnt

K_{Ei}, T_{Ei} = Exciter Gain and Time constant

R_{fi} = Exciter Rate feedback

V_{refi} = Reference Voltage Setting

V = Generator Terminal voltage.

vi) Network equations :

Load-flow equations decide the operating point in terms of bus voltage and phase angle $(V\angle\theta)$ for specified generation schedule and load dispatch.

The steady-state load-flow equations can be written as:

$$0 = -P_i - jQ_i + \sum V_i V_k Y_{ik} \exp\left(j\left(\theta_i - \theta_k - \alpha_{ik}\right)\right) \qquad \ldots\ldots \text{(2.10)}$$

where,

$P_i + jQ_i$ = Real and reactive power injected in the network at bus i.

$Y_{ik}\angle\alpha_{ik}$ = Network Admittance between busses i & k.

$V_i\angle\theta_i$ = Voltage and phase at bus i.

From Eq. (2.6) the injected real and reactive power at the generator buses is given as,

$$P_i + jQ_i = V_i\left(I_{di} - jI_{qi}\right)e^{j\left(\pi/2 + \theta_i - \delta_i\right)} - P_{Li}\left(V_i\right) - jQ_{Li}\left(V_i\right) \qquad \ldots\ldots \text{(2.11a)}$$

Similarly, at the load buses, for $i = m+1,\ldots,n$ we have,

$$P_i + jQ_i = -P_{Li}\left(V_i\right) - jQ_{Li}\left(V_i\right) \qquad \ldots\ldots \text{(2.11b)}$$

22

Combining Eqs.(2.11a) & (2.11b) with Eq.(2.10), for generator buses, the loadflow equation becomes,

$$0 = V_i \left(I_{di} - jI_{qi} \right) e^{j\left(\frac{\pi}{2} + \theta_i - \delta_i\right)} - P_{Li}(V_i) - jQ_{Li}(V_i) - \sum_{k=1}^{n} V_i V_j Y_{ik} e^{j(\theta_i - \theta_i - \alpha_{ik})} \qquad \dots (2.12a)$$

and for load busses, these are,

$$0 = -P_{Li}(V_i) - jQ_{Li}(V_i) - \sum_{k=1}^{n} V_i V_j Y_{ik} e^{j(\theta_i - \theta_i - \alpha_{ik})} \qquad \dots (2.12b)$$

2.6 Stability and Bifurcation

Power System network is a highly non-linear system. Unlike the linear systems, the stability of a non-linear system is a localized concept. The system behaviour depends upon the point of operation. The same system may be stable for a given set of operating points while being unstable at others. The local stability of such systems can be evaluated by eigenvalue analysis of the system dynamic equations around the operating point. The system equations, both the dynamic and algebraic, are linearized around the operating point for this purpose. If all the eigenvalues have negative real part, the system is asymptotically stable in the neighbourhood. If a complex pair of eigenvalues has zero real part, the system is marginally stable and it may exhibit limit cycles. If, on the other hand, any of the eigenvalues has positive real part, the system is unstable.

According to Cutsem [5], '*a bifurcation occurs at any point in parameter space, for which the qualitative structure of the system changes for a small change in parameter vector, 'p.'* The change may be in one of the following :

1. Number of equilibrium points
2. Number of limit cycles
3. Stability of equilibrium points or limit cycles or
4. Period of periodic solution.

Bifurcation theory deals with the sudden change in the eigenvalues as certain system parameter called the loading or bifurcation parameter (say p), is increased. The change may be brought about by merging together of two distinct equilibrium points – one stable and the other unstable (Saddle Node Bifurcation) or by a pair of complex conjugate eigenvalues

23

crossing the imaginary axis (Hopf Bifurcation). There are other forms of bifurcations, like fork-pitch bifurcations and trans-critical bifurcation. Here only saddle node bifurcation and the Hopf bifurcation are dealt with.

2.6.1 Saddle Node Bifurcation

Saddle node bifurcations are characterized by the merging of two equilibrium points of the system dynamic and algebraic equations, typically one stable equilibrium point (s.e.p.) and the other unstable equilibrium point (u.e.p.). At this point, an eigenvalue of the system Jacobian becomes zero. If the two merging equlibria exist for $p < p_o$, then both the equilibrium points disappear for $p > p_o$, and vice-versa. In power system, saddle node bifurcation is indicated by the non-convergence of the load-flow algorithm at the critical point pertaining to one of its eigenvalues becoming zero.

2.6.2 Hopf Bifurcation

Hopf bifurcation is characterized by a pair of complex conjugate eigenvalues for an equilibrium point crossing the imaginary axis of the complex plane. When the bifurcation parameter, p, changes the complex pair move away from the imaginary axis, either to the right or to the left of the axis. Consequently stable or unstable limit cycles (system oscillations) may appear or disappear. Depending upon the stability of these limit cycles and where they occur with respect to the bifurcating parameter p, sub-critical or super-critical Hopf bifurcation occurs.

2.7 System Linearization and Eigen Value Analysis

Power System is described by a set of dynamic and algebraic equations as already described. The complex algebraic equations have to be separated into real and imaginary parts. Symbolically these Differential Algebraic equations (DAE) can be denoted in brief as :

$$\dot{x} = f(x, y) \qquad \ldots\ldots (2.13)$$
$$0 = g(x, y) \qquad \ldots\ldots (2.14)$$

where,

x = vector of dynamic state variables

$$= \begin{bmatrix} \delta & \omega & E'_q & E'_d & E_{fd} & V_R & R_f & T_M \end{bmatrix}^t$$

y = vector of algebraic variables

$$= \begin{bmatrix} i_q & i_d & V & \theta \end{bmatrix}^t$$

Eq (2.13) represents the set of dynamic equations and consists of Eqs. (2.1) to (2.4), Eqs. (2.7) and (2.9), while Eq. (2.14) represents the set of algebraic equations. These algebraic equations consist of Eqs.(2.5) and (2.12); separated into real and imaginary parts. The algebraic variables, denoted by the vector y, depend upon the loading parameter, p. In a power system let a parameter vector p give the specified generation schedule and load dispatch (the change from the base case). Solution of these sets of equations at $\dot{x} = 0$, then defines the initial operating point (x_0, y_0). The linearized equations for the incremental changes in variables over their initial values can be written as,

$$\Delta\dot{x} = A\Delta x + B\Delta y \qquad \ldots (2.15)$$
$$0 = C\Delta x + D\Delta y \qquad \ldots (2.16)$$

where,

$$A = \left[\frac{\partial f}{\partial x}\right]_{x_0, y_0} \qquad , \quad B = \left[\frac{\partial f}{\partial y}\right]_{x_0, y_0} \quad ,$$

$$C = \left[\frac{\partial g}{\partial x}\right]_{x_0, y_0} \qquad \text{and, } D = \left[\frac{\partial g}{\partial y}\right]_{x_0, y_0} .$$

Solving for the value of vector, Δy, from Eq. (2.16) and substituting it in Eq. (2.15) gives,

$$\Delta y = \mathbf{D}^{-1}\mathbf{C}\Delta x$$
$$\therefore \Delta \dot{x} = \left(\mathbf{A} - \mathbf{B}\mathbf{D}^{-1}\mathbf{C}\right)\Delta x \qquad \qquad \text{.... (17)}$$
$$\text{where, } \tilde{\mathbf{A}} = \left(\mathbf{A} - \mathbf{B}\mathbf{D}^{-1}\mathbf{C}\right) \text{ is known as the reduced system Jacobian.}$$

The eigen-value analysis of reduced system Jacobian $\tilde{\mathbf{A}}$ has been used to find out the occurrence of Hopf bifurcation. Saddle node bifurcation is identified by the non-convergence of Newton-Raphson load-flow algorithm.

A flow-chart, given in Fig 2.7 outlines the algorithm the algorithm adopted for the prediction of Hopf and saddle node bifurcation corresponding to parameter changes.

The following assumptions have been considered in the simulation:

1. The reactive power limits of the generator and also the voltage regulator limits of the exciter have not been considered.

2. The line thermal limits have not been considered in the ATC calculations.

3. Load dynamics have been ignored. Only static models of loads have been considered..

4. Change in real power loss due to change in loads and generation is assumed to be supplied by the slack bus generator.

2.8   Simulation Results

A WSCC 3-machine, 9-bus system (described in Appendix A) and another New England 39-bus, 10-generator system (given in Appendix B) have been taken as test systems for the present studies. Some typical transactions were considered between one of the load buses in the system and different generator buses. Saddle node bifurcation (SNB) and Hopf bifurcation (HB) limits have been used for determination of ATC. The ATC value corresponding to the HB gives the dynamic ATC whereas that corresponding to the SNB provides the static ATC. In addition to these, the bus voltage limits have also been considered. Voltage limits are considered at $\pm 10\%$ from the nominal value (1pu). Apart from the values of TTC and ATC, the system real and reactive power losses and the low voltages in the system have also been considered in each case. The ATC and TTC have been computed in terms of only real power transactions expressed in p.u.
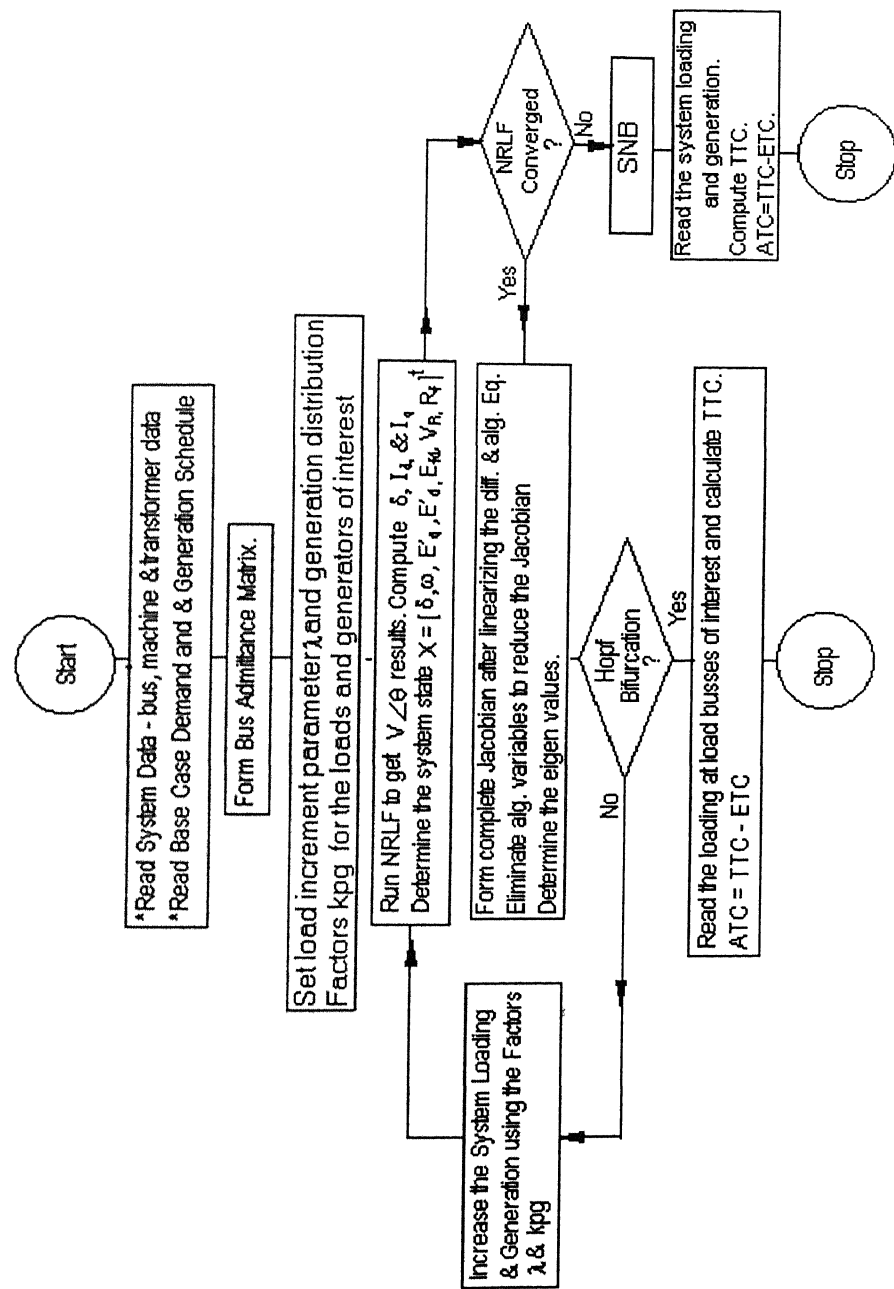
Fig. 2.7 Flow Chart of the Algorithm

Start

*Read System Data - bus, machine & transformer data
*Read Base Case Demand and & Generation Schedule

Form Bus Admittance Matrix.

Set load increment parameter λ and generation distribution Factors kpg for the loads and generators of interest

Run NRLF to get $V \angle \theta$ results. Compute δ, I_d & I_q Determine the system state $X = [\delta, \omega, E'_q, E'_d, E_{fd}, V_R, R_f]^t$

NRLF Converged ?

SNB

Read the system loading and generation. Compute TTC. ATC=TTC-ETC.

Stop

Form complete Jacobian after linearizing the diff. & alg. Eq. Eliminate alg. variables to reduce the Jacobian Determine the eigen values.

Hopf Bifurcation ?

Increase the System Loading & Generation using the Factors λ & kpg

Read the loading at load busses of interest and calculate TTC. ATC = TTC - ETC

Stop

Yes

No

No

Yes

27

For ATC determination, the loading at the selected bus has been increased in the following two distinct ways :

i. **Load1** – In the first case, only the real part of the load is increased while the reactive part is assumed to remain constant. Such a case is referred in the following sections as 'Load1'. This situation may arise in a deregulated market if the consumer locally arranges for the reactive power requirement.

ii. **Load2** – In the second case, both real and reactive parts of the load has been increased in the same proportion such that the load power factor remains constant. This is referred as 'Load2' in the following sections. This case refers to a situation in deregulated market, when consumers also purchase the reactive power from the market.

In both the cases the real power output of generators participating in the transaction has been increased by the amount of load change in the ratio of predefined generation distribution factors. The slack bus generator is assumed to supply the change in system loss. The results for the two systems are described below.

2.8.1   WSCC 3-machine, 9-bus System

The system data, one line diagram and the base-case results are given in Appendix A. With the system load being increased at bus 5, the following transactions have been considered:

i)   Transaction 'T1'

Generator 1 alone supplies the increase in load at bus 5.

ii) Transaction 'T2'

Generator 2 alone supplies the increase in load at bus 5.

iii) Transaction 'T3'

Generator 3 alone supplies the increase in load at bus 5.

iv) Transaction 'T4'

Generators at buses 1 and 2 equally share the increase in load at bus 5.

v) Transaction 'T5'

        Generators at buses 2 and 3 equally share the increase in load at bus 5.

vi) Transaction 'T6'

        Generators at buses 1 and 3 equally share the increase in load at bus 5.

vii) Transaction 'T7'

        Generators at buses 1, 2 and 3 are supplying the increased load in the ratio of 0.65, 0.25 and 0.10 respectively, chosen in approximate proportion to their respective machine inertia.

The results of the dynamic ATC determination for 'Load1' case are shown in Table 2.1 for all the transactions defined above. Only Hopf bifurcation limits were considered in this case. Along with the values of TTC and ATC, the real and reactive power losses and the critical buses with minimum voltage magnitude in the system are shown.

Table 2.1
Dynamic ATC using Hopf Bifurcation Criteria - Load1 Case
(WSCC 3-machine, 9-bus System)

Transactions	Load	ATC	Ploss	Qloss	Low Voltage Profile		
					V_4	V_5	V_6
Base Case	1.25	-	0.046	-0.922	1.026	0.996	1.013
T1	4.60	3.35	0.256	2.078	0.947	0.848	0.952
T2	3.55	2.30	0.349	1.870	0.972	0.868	0.959
T3	3.50	2.25	0.326	1.398	0.974	0.896	0.948
T4	4.30	3.05	0.285	1.579	0.970	0.866	0.966
T5	3.85	2.60	0.381	1.79	0.964	0.863	0.945
T6	4.40	3.15	0.300	1.630	0.963	0.865	0.954
T7	4.40	3.15	0.249	1.371	0.970	0.866	0.966

Table 2.2 shows the values of ATC, TTC, system losses and bus voltages having lowest values at the critical loading level when Saddle Node Bifurcation is observed.

Table 2.2
Static ATC using Saddle Node Bifurcation Criteria – Load1 Case
(WSCC 3-machine, 9-bus System)

Transactions	Load	ATC	Ploss	Qloss	Low Voltage Profile		
					V_4	V_5	V_6
Base Case	1.25	-	0.046	-0.922	1.026	0.996	1.013
T1	5.15	3.90	0.487	4.977	0.863	0.702	0.883
T2	4.35	3.10	0.709	5.312	0.903	0.709	0.892
T3	4.75	3.50	0.857	6.317	0.866	0.691	0.816
T4	5.25	4.00	0.570	4.575	0.894	0.707	0.904
T6	4.70	3.45	0.749	4.955	0.890	0.704	0.868
T7	5.40	4.15	0.543	4.625	0.879	0.695	0.897

Tables 2.3 & 2.4 show the results for the ATC values when both the real and reactive loading is simultaneously increased (Load2). It is observed that the ATC values are lower in 'Load2' case as compared to 'Load1' case. Moreover, 'Load2' case results in poorer voltage profile.

Table 2.3
Dynamic ATC using Hopf Bifurcation Criteria – Load2 Case
(WSCC 3-machine, 9-bus System)

Transaction	Load	ATC	Ploss	Qloss	Min Voltage Profile		
					V_4	V_5	V_6
Base Case	1.25	-	0.046	-0.922	1.026	0.996	1.013
T1	2.35	1.10	0.201	0.964	0.918	0.713	0.928
T2	2.25	1.00	0.265	1.386	0.915	0.705	0.921
T3	2.25	1.00	0.245	1.075	0.918	0.721	0.921
T4	2.35	1.10	0.239	1.226	0.913	0.698	0.922
T5	2.25	1.00	0.249	1.133	0.918	0.716	0.922
T6	2.35	1.10	0.230	1.081	0.914	0.705	0.923
T7	2.35	1.10	0.221	1.068	0.916	0.706	0.925

Table 2.4
Dynamic ATC using saddle Node Bifurcation Criteria - Load2 Case
(WSCC 3-machine, 9-bus System)

Transaction	Load	ATC	Ploss	Qloss	Min Voltage Profile		
					V_4	V_5	V_6
Base Case	1.25	-	0.046	-0.922	1.026	0.996	1.013
T1	2.58	1.33	0.325	2.297	0.874	0.605	0.894
T2	2.45	1.20	0.404	2.792	0.873	0.598	0.886
T3	2.52	1.27	0.469	3.291	0.850	0.548	0.862
T4	2.55	1.30	0.372	2.600	0.870	0.588	0.888
T5	2.50	1.25	0.429	2.905	0.862	0.575	0.876
T6	2.58	1.33	0.389	2.718	0.862	0.572	0.881
T7	2.58	1.33	0.368	2.593	0.867	0.582	0.886

Further, the values of ATC for the defined transactions were computed considering the voltage limits apart from the bifurcation limits. The results are given in Table 2.5.

Table 2.5
ATC Value Determination on the Basis of Voltage Limit Criteria
(WSCC 3-machine, 9-bus System)

Transaction	Load1	ATC1	Load2	ATC2
Base Case	1.25	-	1.25	-
T1	4.03	2.78	1.45	0.20
T2	3.23	1.98	1.40	0.15
T3	3.48	2.23	1.40	0.15
T4	3.85	2.60	1.40	0.15
T5	3.43	2.18	1.40	0.15
T6	3.93	2.68	1.40	0.15
T7	4.00	2.75	1.40	0.15

The ATC values obtained while considering the different limits viz. - Voltage, Hopf bifurcation and saddle node bifurcation are depicted in the charts in Fig. 2.8 & 2.9. Due to excessive reactive power loading, the ATC values are much lower when voltage limits are considered than those in the previous cases corresponding to only bifurcation limits.
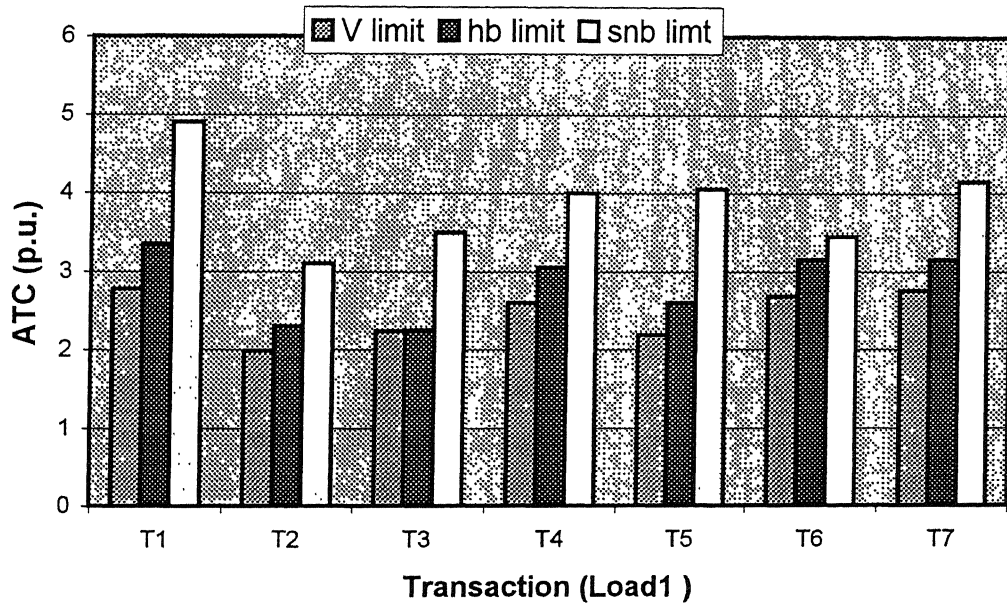
Fig. 2.8 ATC for WSCC 9-Bus System -Load1 Case.
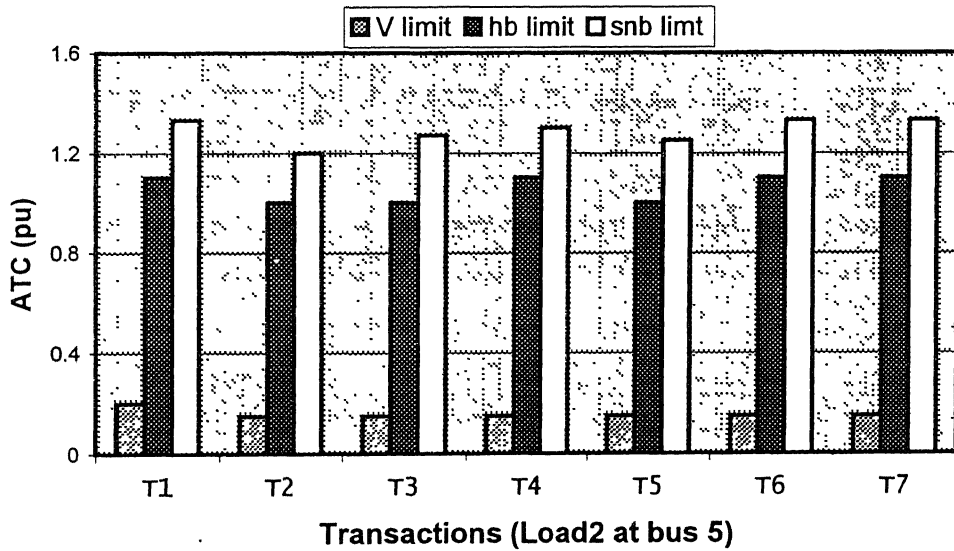
Fig. 2.9 ATC for WSCC 9-Bus System -Load2 Case.

2.8.2   39-bus, 10-Generator System

Details of this system, its one-line diagram and the base case load-flow results are given in Appendix B. Following transactions were studied between load bus 18 and the specified seller (generator) buses:

i)   Transaction 'T1'

Generator 1 alone supplies the increase in load at bus 18.

ii) Transaction 'T2'

Generator 2 alone supplies the increase in load at bus 18.

iii) Transaction 'T3'

Generator 3 alone supplies the increase in load at bus 18.

iv) Transaction 'T4'

Generator 8 alone supplies the increase in load at bus 18.

v)   Transaction 'T5'

Generator 10 alone supplies the increase in load at bus 18.

The results of ATC calculation based on Hopf and saddle node bifurcations and after considering the minimum voltage limits are given in Tables 2.6 to 2.10.

Table 2.6 shows the results corresponding to Load1 case and only Hopf bifurcation limit. The system losses and low voltage at the few weak buses are included.

Table 2.6
Dynamic ATC using Hopf Bifurcation Criteria - Load1 Case
(39-bus, 10-Generator System)

Transaction	Load	ATC	Ploss	Qloss	Low Voltage Profile				
					V_{15}	V_{16}	V_{17}	V_{18}	V_{32}
Base Case	5.22	-	0.482	0.045	0.947	0.948	0.940	0.941	0.931
T1	14.62	9.40	0.658	9.135	0.897	0.899	0.885	0.983	0.896
T2	22.45	17.23	1.453	18.385	0.856	0.863	0.828	0.817	0.868
T3	17.75	12.53	1.083	18.111	0.855	0.858	0.841	0.842	0.837
T4	12.53	7.31	1.230	7.808	0.922	0.925	0.914	0.913	0.912
T5	21.92	16.70	1.595	25.727	0.853	0.861	0.838	0.835	0.859

The results for the TTC and ATC considering the Saddle Node Bifurcation limit for Load1 case are given in Table 2.7.

Table 2.7
Static ATC using Saddle Node Bifurcation Criteria– Load1 Case
(39-bus, 10-Generator System)

Transaction	Load	ATC	Ploss	Qloss	Low Voltage Profile				
					V_{15}	V_{16}	V_{17}	V_{18}	V_{32}
Base Case	5.22	-	0.482	0.045	0.947	0.948	0.940	0.941	0.931
T1	20.88	15.66	1.097	29.849	0.777	0.776	0.754	0.756	0.811
T2	25.58	20.36	2.256	33.812	0.778	0.789	0.731	0.711	0.813
T3	21.40	16.18	1.765	38.436	0.746	0.749	0.724	0.725	0.722
T4	26.62	21.40	6.627	70.038	0.718	0.733	0.690	0.686	0.756
T5	27.14	21.92	3.121	58.883	0.714	0.731	0.684	0.677	0.752

For the cases when both real and reactive power at bus 18 is increased, the ATC values determined on the basis of Hopf bifurcation and saddle node bifurcation limits are shown in Tables 2.8 and 2.9.

Table 2.8
Dynamic ATC using Hopf Bifurcation Criteria-Load2 Case
(39-bus, 10-Generator System)

Transaction	Load	ATC	Ploss	Qloss	Low Voltage Profile				
					V_{15}	V_{16}	V_{17}	V_{18}	V_{32}
Base Case	5.22	-	0.482	0.045	0.947	0.948	0.940	0.941	0.931
T1	15.14	9.92	0.769	12.924	0.844	0.848	0.818	0.811	0.861
T2	16.18	10.96	0.796	13.635	0.835	0.839	0.807	0.799	0.855
T3	16.18	10.96	0.840	14.827	0.829	0.833	0.800	0.792	0.829
T4	16.18	10.96	0.868	14.529	0.832	0.837	0.803	0.795	0.853
T5	16.18	10.96	0.816	14.156	0.834	0.838	0.804	0.797	0.854

Table 2.9
Dynamic ATC using Saddle Node Bifurcation Criteria-Load2 Case
(39-bus, 10-Generator System)

Transaction	Load	ATC	Ploss	Qloss	Low Voltage Profile				
					V_{15}	V_{16}	V_{17}	V_{18}	V_{32}
Base Case	5.22	-	0.482	0.045	0.947	0.948	0.940	0.941	0.931
T1	18.27	13.05	1.157	28.092	0.740	0.744	0.698	0.688	0.788
T2	19.31	14.09	1.251	30.394	0.718	0.723	0.671	0.659	0.773
T3	18.79	13.57	1.211	28.258	0.736	0.741	0.692	0.681	0.784
T4	18.79	13.57	1.202	26.520	0.749	0.754	0.707	0.696	0.795
T5	18.79	13.57	1.263	25.698	0.753	0.758	0.711	0.700	0.798

Table 2.10 shows the ATC values considering the minimum voltage limits for both types of load increase viz. 'Load1' and 'Load2' cases.

Table 2.10
ATC Value determination on the basis of Voltage limit criteria
(39-bus, 10-generator system)

Transaction	Load1	ATC1	Load2	ATC2
Base Case	5.22	-	5.22	-
T1	13.05	7.83	9.92	4.70
T2	14.09	8.87	9.92	4.70
T3	13.57	8.35	9.92	4.70
T4	13.57	8.35	9.92	4.70
T5	13.57	8.35	9.92	4.70

The charts given in Fig. 2.10 compares the ATCs obtained for different limits when only the real power demand at bus 18 is increased, while Fig. 2.11 compares the ATC for different limiting cases when both real and reactive power are increased.
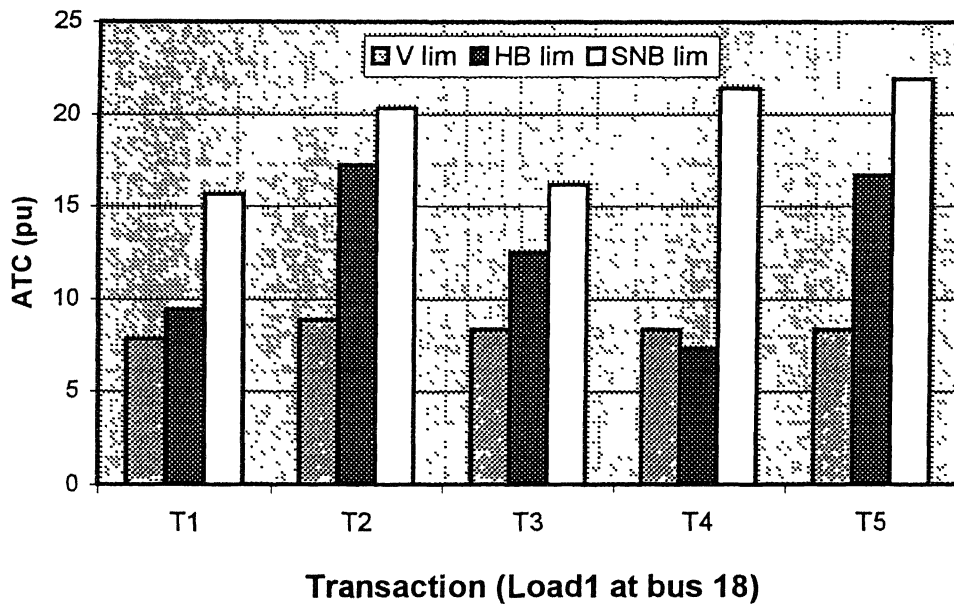
Transaction (Load1 at bus 18)
Fig. 2.10 ATC for 39 Bus System - Load1 Case
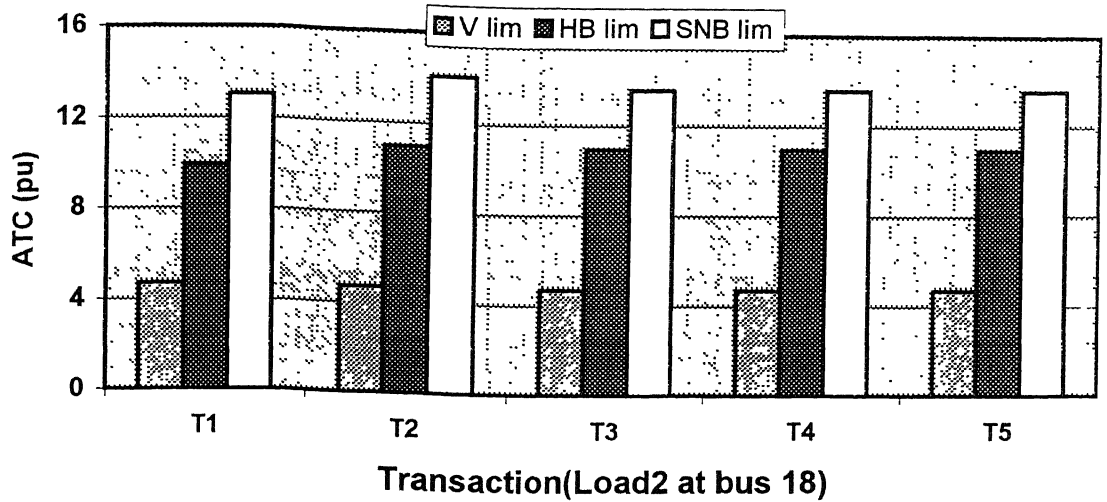
Fig. 2.11 ATC for 39 Bus System- Load2 Case

It is interesting to note that in almost all cases the ATC is minimum when voltage limit is imposed except the 'Load1' and transaction T4 case in 39-bus system when the ATC with only HB limit is the minimum.

2.8.3 Effect of load modelling

The simulation results for ATC calculation was also obtained for the WSCC system using the static voltage dependent load model. These are given in Tables 2.11 and 2.12 for the 'Load1' and 'Load2' cases respectively. The expressions for such a model, also known as ZIP model, is given by

$P_L = P_L(ap+bpV^2+cpV)$ and $Q_L = Q_L(aq+bqV^2+cqV)$.

For the present study load coefficients were assumed as ap = 0.6, bp=0.2, cp=0.2, aq=0.4, bq=0.3 and cq=0.3 to reflect a hypothetical case.

A comparison of ATC values in Tables 2.11 and 2.12 with those in Tables 2.11 and 2.12 reveals that ATC values are higher when voltage dependent models of loads are considered.

36

Table 2.11
ATC Values for ZIP Load model – Load1 Case
$P_L= P_L(0.6+0.2V^2+0.2V), \quad Q_L= Q_L(0.4+0.3V^2+0.3V)$
(WSCC 3-machine, 9-bus System)

Transaction	Hopf Bif.		SN Bif.		LV limit	
	Load	ATC	Load	ATC	Load	ATC
T1	5.28	4.03	5.20	3.95	4.12	2.87
T2	3.46	2.21	3.91	2.66	3.15	1.90
T3	**3.40**	**2.15**	**4.27**	**3.02**	**3.44**	**2.19**
T4	5.09	3.84	5.14	3.89	3.86	2.61
T5	4.17	2.92	4.25	2.99	3.37	2.12
T6	5.16	3.91	5.32	4.07	3.98	2.73
T7	5.47	4.22	5.46	4.21	4.07	2.82

Comparing the results in Table 2.11 for the voltage dependent ZIP load model with Table 2.1 for constant power model, it is observed that the ATC values are different but they do not follow any specific pattern.

Table 2.12
ATC Values for ZIP Load model – Load2 Case
$P_L= P_L(0.6+0.2V^2+0.2V), \quad Q_L= Q_L(0.4+0.3V^2+0.3V)$
(WSCC 3-machine, 9-bus System)

Transaction	Hopf Bif.		SN Bif.		LV limit	
	Load	ATC	Load	ATC	Load	ATC
T1	-	-	2.87	1.62	1.46	0.21
T2	2.500	1.25	2.48	1.23	1.41	0.16
T3	2.64	1.39	2.63	1.38	1.45	0.21
T4	-	-	2.74	1.49	1.46	0.21
T5	-	-	2.56	1.31	1.41	0.16
T6	-	-	2.80	1.55	1.46	0.21
T7	-	-	2.81	1.56	1.46	0.21

In Table 2.12, Hopf bifurcation is occurring only in transactions T2 and T3. This may be explained by the decrease in the constant impedance and constant current components of the load, as voltage drops to lower value. It is interesting to note in Table 2.12 that the ATC value corresponding to the saddle node bifurcation limit is slightly less than the ATC value corresponding to the Hopf bifurcation when voltage dependent ZIP load model is considered.

2.9 Conclusions

This chapter has presented a methodology for dynamic and static ATC determination based on Hopf and saddle node bifurcation limits, in addition to the bus voltage limits. The study results obtained on 9-bus WSCC and 39-bus New England systems provide the following conclusions :

I. Hopf bifurcation occurred before the saddle node bifurcation in all the cases considered. This resulted in lower values of dynamic ATC (corresponding to HB) than the static ATC (corresponding to SNB).

II. The ATC values were considerably less when both real and reactive power loads were increased (Load2 case) in comparison to corresponding increase of only real power loads (Load1 case).

III. Consideration of voltage limits resulted in lower value of ATC as compared to the values obtained with the bifurcation limits alone in most of the cases. In few cases, e g transaction T4 in 39-bus system (Load1 case) with constant power load model and transaction T3 in 9-bus system (Load1 case) with voltage dependent load model, the ATC with Hopf bifurcation limit was found to be the minimum most.

IV. Both real and reactive power losses increase with the increase in loading. These were found high when only saddle node bifurcation limits were considered. For the same ATC value losses may differ. For instance, transactions T4 and T5 in 39-bus system (Table 2.7) result in similar ATC values, but the losses for the transaction T4 were much greater than those for T5.

CHAPTER 3

SVC PLACEMENT FOR ENHANCEMENT OF ATC

3.1 Introduction

In chapter-2, bifurcation concept was used to determine Available Transfer Capability (ATC) of the transmission networks. Hopf bifurcation and saddle node bifurcation criteria along with the bus voltage limits were utilized to determine dynamic ATC and static ATC, respectively. In almost all the cases considered for the study, it was found that the minimum voltage limit is the limiting constraint. An increase in system loading, in terms of both real and reactive power, means higher line currents and higher voltage drop in line impedances. It is the excessive voltage drops in line reactances, which result in voltage decline and increase in transmission losses at heavy loadings. By the same logic, voltage rise may be observed when the system is lightly loaded.

Reactive power compensation and management [2,6,7,8] has been known to improve system voltage profile. A wide variety of reactive power compensation devices and schemes have been developed and installed throughout the world. Static Var Compensator (SVC) is a power-electronics based device developed as one of the Flexible Transmission System (FACTS) controllers. It is expected that introduction of SVC in power system will enhance the ATC values. This chapter presents a scheme for optimal placement of SVC based on the eigenvalue analysis and maximum participation factor. The impact of placement of SVC on the enhancement of ATC values has been studied on the WSCC 9-bus, 3-machine and New England 39-bus, 10-generator systems.

3.2 Static Var Compensator

According to ref [2], Static Var Compensator (SVC) is –

"A shunt-connected static Var generator or absorber whose output is adjusted to exchange capacitive or inductive current as to maintain or control specific parameters of the power system (typically bus voltage)."

SVC, thus, regulates the system voltage by injecting the required amount of reactive power (Var) in the system. It includes separate equipments for leading and lagging Vars – the thyristor controlled reactors (TCR) for absorbing reactive power and thyristor switched capacitor (TSC) banks for supplying the reactive Var. Fig. 3.1 shows a typical scheme of SVC. Depending upon the size and requirement, it may also include fixed or mechanically switched capacitors and reactors. For smooth voltage control, the rating of the TCR is slightly higher than that of a discrete TSC (or fixed Capacitor – FC) block. The harmonic filters employed in SVC are capacitive at fundamental frequency, supplying reactive power of the order of 10-30% of the TCR rating.
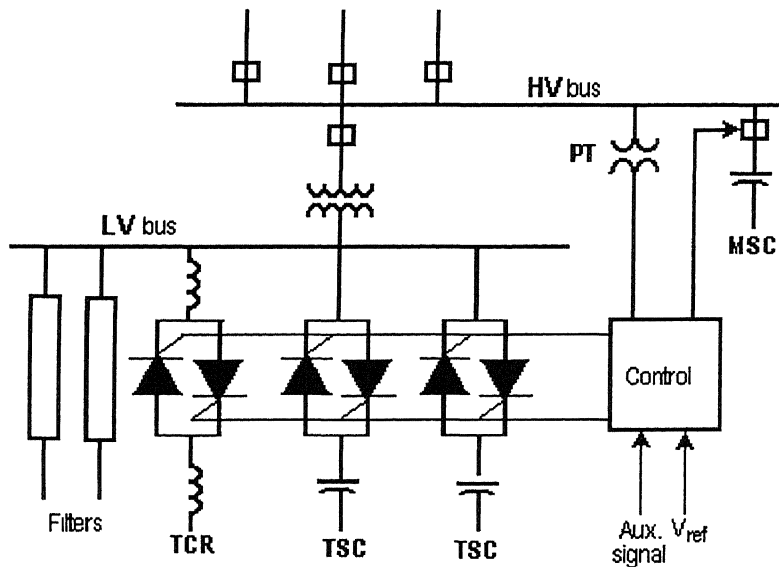
Fig 3.1 A Typical SVC Scheme [27]

When bus voltage drops, the error in bus voltage from the desired value is computed and the value of required capacitive current is determined. Assuming that the TCR is at minimum (zero) conductance level, the capacitor has to be switched for Var generation. Transient free switching of the TSC is achieved if it is switched at certain instants. When the residual voltage across the capacitor is lower than the system peak voltage, it should be switched at the instant when the system voltage equals the capacitor voltage. When the residual capacitor voltage is larger than the system peak voltage, it should be switched at the instant of occurrence of peak system voltage. In both the cases, the voltage appearing across

the thyristor at the instant of firing is minimum. If the voltage starts rising, the TCR conduction period is increased so that it results in an increase in Var consumption and voltage rise is controlled.

In the active control range, the susceptance (B_{svc}), and hence the reactive current, is varied according to the voltage regulation slope characteristics (Fig. 3.2). The slope value depends upon the desired voltage regulation, the desired sharing of reactive power among various sources and other needs in the system. Typically, it varies between 1-5%. It behaves like a shunt capacitor of maximum value (B_{Csvc}) at the capacitive limit, and as fixed shunt reactor at minimum value ($-B_{Lsvc}$) corresponding to the inductive limit. The limits are reached when there are large variations in the bus voltage. Inductive limit is reached when the bus voltage exceeds the upper limit; capacitive limit when it falls below the lower limit.
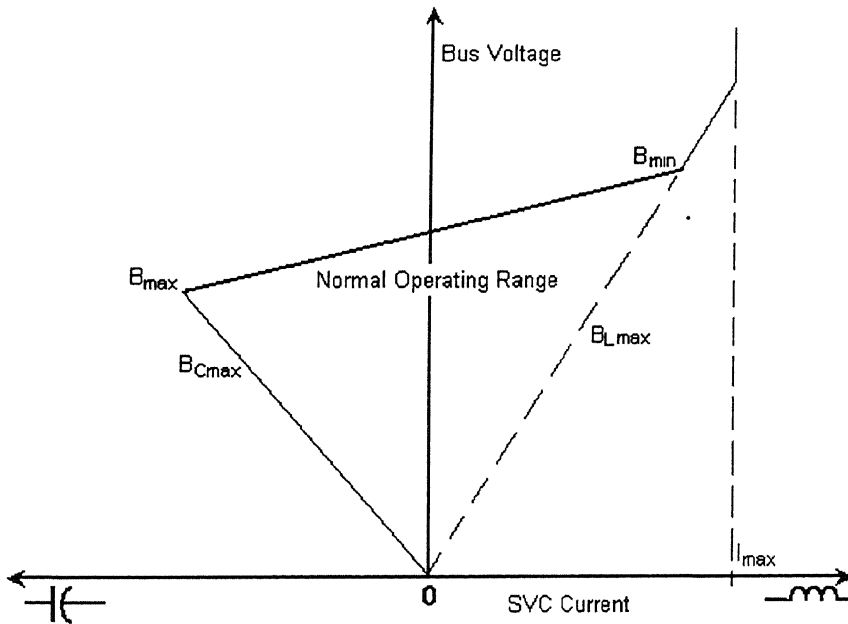
Fig. 3.2 SVC Output characterics

3.3 Dynamic Model of SVC

Fig. 3.3 gives a block diagram representation of SVC, taken from refs [16,27]. The measurement module for sensing the voltage and converting it into dc feedback signal has been ignored as it has small time constant. Further, in this work, the upper and lower limits of the SVC have been ignored. The gain, K_R, is the reciprocal of the slope setting. K_R is

41

usually between 20 per unit (5% slope) and 100 per unit (1% slope) on the SVC base. The regulator time constant, T_R is usually between 20 and 150 milliseconds.
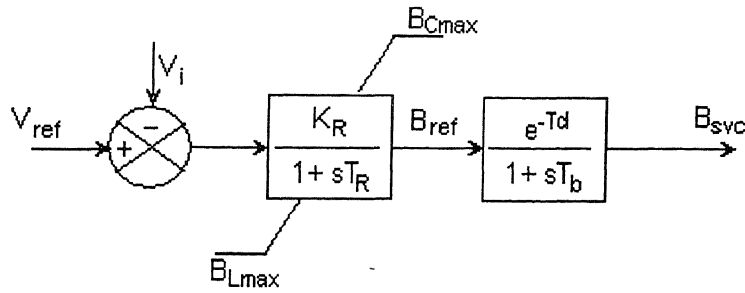
Fig 3.3 Dynamic Model of SVC

The time constant T_d is due to the time lag in the application of firing pulses corresponding to the new value of B_{svc}. T_b is the firing circuit time constant representing the effect of firing sequence and is typically of the order of $3 - 6$ ms. The limits B_{Cmax} and B_{Lmax} correspond to the upper and lower limits of the SVC. The dynamic equations can be written as :

$$T_R \dot{B}_{ref} = -B_{ref} + K_R \left(V_{ref} - V_i \right) \qquad ....(3.1)$$

$$T_b \dot{B}_{svc} = -B_{svc} + B_{ref} \qquad .....(3.2)$$

At steady state,

$$B_{svc} = B_{ref} = K_R \left(V_{ref} - V_i \right)$$

$$\text{and } Q_{svc} = V_i^2 \, B_{svc} \qquad .....(3.3)$$

Reactive power equations at a SVC bus 'm' can be written in a modified form as follows :

$$Q_m = V_m \sum_{k=1}^{n} Y_{mk} V_k \sin\left(\theta_m - \theta_k - \alpha_{mk} \right) - V_m^2 \cdot B_{svc} \qquad ....(3.4)$$

To include SVC in the load-flow mode, the elements of the sub-matrix J_4 of Newton-Raphson loadflow Jacobian, $[J] = \begin{bmatrix} J1 & J2 \\ J3 & J4 \end{bmatrix}$ will be modified as:

42

$$J4(m,m) = J4(m,m) - 2 \cdot V_m K_R \left(V_{ref} - \frac{3}{2} V_m \right) \qquad \dots (3.5)$$

$$\text{where, } [J4] = \frac{\partial Q_m}{\partial V_m} . V_m \bigg|_{(V,\theta)}$$

3.4 Optimal SVC Placement Criterion

In the present work, the state participation factor analysis [16] corresponding to the critical modes responsible for the Hopf Bifurcation (or saddle node bifurcation) has been used for placement of SVC. SVC has been placed at a load bus having maximum voltage state participation corresponding to the critical mode. For this purpose, complete Jacobian, which contains the elements corresponding to all the dynamic and algebraic variables, has to be analyzed. Participation factors have been computed by a method described by Kundur [7]. Corresponding to a given critical eigenvalue, λ_i, the right eigen-vector, ϕ_i, gives the *mode shape*, i.e. the relative activity of the state variables when the particular mode is excited Similarly, the left eigen-vector, ψ_i, identifies the combination of original state variables that displays in the i-th mode corresponding to the eigen-value, λ_i. The k-th element of the right eigen vector, ψ_i, measures the activity of the variable x_i in the i-th mode, and the k-th element of the left eigen vector, ϕ_i, weighs the contribution of this activity to the i-th mode. If, corresponding to the critical eigen-value, λ_i, ϕ_i and ψ_i are the normalized right and left eigen-vectors respectively, the vector of participation factors for different variables is given by,

$$PF_i = \sum_{k=1}^{nv} \phi_{ik} \cdot \psi_{ki} \qquad \dots (3.6)$$

Bus state participation factors identify the buses associated with each mode. The sum of all the participation factors is unity when the right and left eigen-vectors are normalized.

For the different transactions and loading cases, described in the last chapter, the participation factors were calculated corresponding to the most critical eigenvalue. The load bus having the maximum voltage state participation factor corresponding to the critical mode was selected for the SVC placement.

43

Following assumptions have been taken in this study regarding the modelling of SVC:

1 The SVC limits were kept floating. The regulation slope was fixed for the different case studies.

2 Time lag in the bus voltage feedback circuit has been assumed to be zero.

3 The losses in the SVC and the coupling transformer have not been considered.

Bus selection for SVC placement :

For each transaction case complete Jacobian matrix was formed as described in chapter2. The critical eigen-value, i.e. the one closest to the imaginary axis on the complex plane, as all the eigenvalues have negative real part in a stable system, was determined and the corresponding participation factors were computed. From these, the participation factors corresponding to only the bus voltage variables were selected and sorted in ascending order and the bus having the maximum participation factor in most of the cases was selected for the placement of SVC.

In order to study the impact of SVC on ATC, the differential equations describing the SVC dynamics were included in the state equations and correspondingly the Jacobian matrix was modified. The load-flow equation corresponding to the SVC bus was also modified to incorporate the reactive power injection characteristic of the SVC. Further, ATC was determined for each case with SVC placed at the selected bus.

3.5 Simulation Results

The impact of SVC placement on ATC was studied on WSCC 9-bus and 39-bus New England systems. In both the systems, a slope of 1% (the SVC output changes by 1 pu for 1% drop in voltage), which corresponds to SVC regulator gain, $K_R=100$, has been considered. V_{ref} for SVC has been taken as 1 pu. T_R and T_b are taken as 50 ms and 6 ms respectively. All the results given below in subsequent sections are in pu.

3.5.1 WSCC 3-machine, 9-bus System

For the different transactions with 'Load1' case studied in chapter-2, the calculated values of load bus voltage participation factors corresponding to the critical eigenvalue are given in Table 3.1 when only Hopf bifurcation (HB) limits were used to compute the ATC. Table 3.2 lists out the participation factors when saddle node bifurcation (SNB) limits were considered.

Table 3.1
Critical Load Bus Voltage Participation Factors for HB Limit -Load1 Case
(WSCC 3-machine, 9-bus system)

T1		T2		T3		T4		T5		T6		T7	
Bus	PF	Bus	PF	Bus	PF	Bus	PF	Bus	PF	Bus	PF	Bus	PF
9	0.0422	9	0.0485	9	0.0470	9	0.0456	9	0.0477	9	0.0458	9	0.0437
8	0.0461	8	0.0518	8	0.0500	8	0.0502	8	0.0523	8	0.0505	8	0.0479
7	0.0551	6	0.0520	6	0.0524	6	0.0581	6	0.0564	7	0.0590	7	0.0569
6	0.0622	4	0.0581	7	0.0551	7	0.0594	7	0.0604	6	0.0612	6	0.0584
4	0.0873	7	0.0583	4	0.0570	4	0.0735	4	0.0644	4	0.0778	4	0.0763
5	**0.1037**	**5**	**0.0734**	**5**	**0.0668**	**5**	**0.0903**	**5**	**0.0818**	**5**	**0.0938**	**5**	**0.0911**

Table 3.2
Critical Load Bus Voltage Participation Factors for SNB Limit -Load1 Case
(WSCC 3-machine 9-bus system)

T1		T2		T3		T4		T5		T6		T7	
Bus	PF	Bus	PF	Bus	PF	Bus	PF	Bus	PF	Bus	PF	Bus	PF
9	0.0325	9	0.0407	9	0.0357	9	0.0305	9	0.0361	9	0.0324	9	0.0310
8	0.0411	8	0.0525	8	0.0497	8	0.0421	8	0.0478	8	0.0439	8	0.0418
7	0.0581	6	0.0666	7	0.0688	6	0.0628	6	0.0685	7	0.0638	7	0.0630
6	0.0667	7	0.0704	6	0.0745	7	0.0646	6	0.0703	6	0.0671	6	0.0643
4	0.1177	4	0.0939	4	0.1043	4	0.1111	4	0.1029	4	0.1147	4	0.1150
5	**0.1975**	**5**	**0.1795**	**5**	**0.1902**	**5**	**0.2222**	**5**	**0.2009**	**5**	**0.2114**	**5**	**0.2155**

In all the cases listed above the voltage at load bus 5 is found to have maximum participation factor to the critical mode. Hence, bus 5 was selected as the optimal location for SVC.

Tables 3.3 and 3.4 show the results of ATC calculated for the 'Load1' case transactions defined already in chapter 2 and also bus voltage profile at few weak buses after the placement of SVC at bus 5.

Table 3.3
Dynamic ATC using Hopf Bifurcation Criteria – Load1 Case
(WSCC 9-bus system with SVC at bus 5)

Transactions	Load	ATC	Ploss	Qloss	Low Voltage Profile		
					V_8	V_5	V_6
Base Case	1.25	-	0.046	-0.929	1.017	0.9996	1.014
T1	7.84	6.59	1.191	15.732	V_4=0.747	0.920	0.779
T2	4.03	2.78	0.393	2.077	0.986	0.985	V_7=0.990
T3	3.59	2.34	0.315	1.162	0.996	0.990	0.976
T4	6.71	5.46	0.569	4.316	0.982	0.972	0.981
T5	5.46	4.21	0.702	3.929	0.974	0.976	0.947
T6	5.90	4.65	0.454	3.052	0.986	0.979	0.969
T7	8.96	7.71	0.984	9.707	V_4=0.903	0.942	0.917

For all the transactions, except transaction – 'T1', the voltage profile at the lowest voltage busses are well above the minimum limit at the occurrence of Hopf Bifurcation The corresponding ATC values are much higher than those for the cases without SVC, shown in Table 2.1.

Table 3.4
Static ATC using Saddle Node Bifurcation Criteria-Load1 Case
(WSCC 3-machine, 9-bus System with SVC at bus 5)

Transactions	Load	ATC	Ploss	Qloss	Low Voltage Profile		
					V_4	V_5	V_6
Base Case	1.25	-	0.046	-0.922	1.026	0.996	1.013
T1	7.90	6.65	0.945	12.182	0.822	0.937	0.846
T2	6.46	5.21	1.764	14.521	V_7=0.756	V_8=0.784	0.894
T3	6.46	5.21	1.592	12.575	V_8=0.790	V_9=0.824	0.731
T4	9.65	8.40	1.922	14.438	0.830	V_7=0.841	0.846
T5	7.72	6.46	2.126	14.756	V_7=0.833	V_8=0.842	0.775
T6	9.28	8.03	1.905	19.755	0.761	V_8=0.814	0.750
T7	9.59	8.34	1.397	14.742	0.820	0.913	0.854

For Saddle node bifurcation limit cases, though the bus-voltages drop below the minimum voltage limit of 0.9 pu at certain buses, the voltage profile is better than those in Table 2.2, without SVC. The ATC values with SNB limits also increase when SVC is placed n the system.

46

The results for the simulations when both real and reactive power load at bus 5 are increased ('Load2' in chapter 2) are shown in Tables 3.5 & 3.6. Comparing the results with those shown in Table 2.3 and 2.4, it is found that ATC values and the voltage profile have improved in 'Load2' case also. The reactive power loss in the base case has slightly reduced with the introduction of SVC.

Table 3.5
Dynamic ATC using Hopf Bifurcation Criteria-Load2 Case
(WSCC 9-bus System with SVC at bus 5)

Transactions	Load	ATC	Ploss	Qloss	Low Voltage Profile		
					V_8	V_5	V_6
Base Case	1.25	-	0.046	-0.929	1.017	0.9996	1.014
T1	7.59	6.34	1.214	15.997	V_4=0.725	0.885	0.759
T2	4.03	2.78	0.397	2.122	0.983	0.974	V_7=0.987
T3	3.59	2.34	0.316	1.188	0.994	0.981	0.973
T4	6.65	5.40	0.573	4.379	0.976	0.949	0.974
T5	5.40	4.15	0.694	3.901	0.971	0.959	0.942
T6	5.90	4.65	0.463	3.159	0.981	0.960	0.963
T7	8.71	7.46	0.974	9.610	V_4=0.891	0.906	0.907

Table 3.6
Static ATC using Saddle Node Bifurcation Criteria-Load2 Case
(WSCC 9-bus System with SVC at bus 5)

Transactions	Load	ATC	Ploss	Qloss	Low Voltage Profile		
					V_4	V_5	V_6
Base Case	1.25	-	0.046	-0.929	V_8=1.017	0.9996	1.014
T1	7.71	6.46	1.083	14.107	0.768	0.895	0.798
T2	6.21	4.96	1.310	10.253	V_7=0.842	V_8=0.860	0.921
T3	6.34	5.09	1.457	11.290	V_9=0.849	V_8=0.816	0.756
T4	8.78	7.53	1.230	11.135	0.909	0.898	V_7=0.905
T5	7.28	6.03	1.641	11.061	V_8=0.885	V_7=0.881	0.828
T6	8.59	7.34	1.233	11.534	0.875	V_8=0.893	0.851
T7	8.78	7.53	1.001	9.934	0.886	0.904	0.903

Table 3.7 presents the ATC values when bus voltage limits are considered for both Load1 and Load2 cases. A comparison of results with those in Table 2.5 shows a distinct improvement in ATC values in this case too.

Table 3.7
ATC Value Determination on The Basis of Voltage Limit Criteria
(WSCC 3-machine, 9-bus System with SVC placed at Bus 5)

Transaction	Load1	ATC1	Load2	ATC2
Base Case	1.25	-	1.25	-
T1	7.46	6.21	7.21	5.96
T2	5.90	4.65	5.78	4.53
T3	5.28	4.03	5.21	3.96
T4	9.28	8.03	8.78	7.53
T5	6.59	5.34	6.40	5.15
T6	8.15	6.85	7.84	6.59
T7	9.03	7.78	8.65	7.40

Figs. 3.4 and 3.5 depict the ATC values of all transactions. While ATC values have increased after the placement of SVC for all the transactions, Hopf bifurcation is found to be the limiting constraint for ATC in most of the cases.
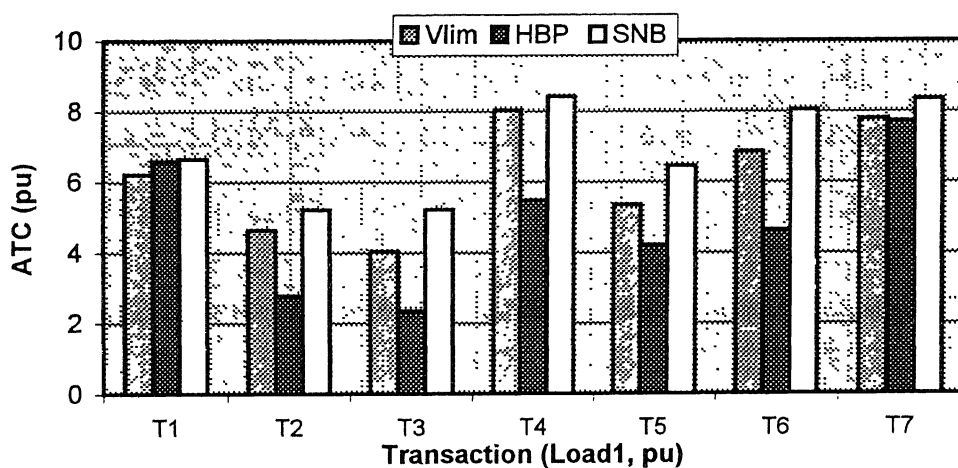
Fig. 3.4 ATC for 9 Bus System with SVC - Load1 Case
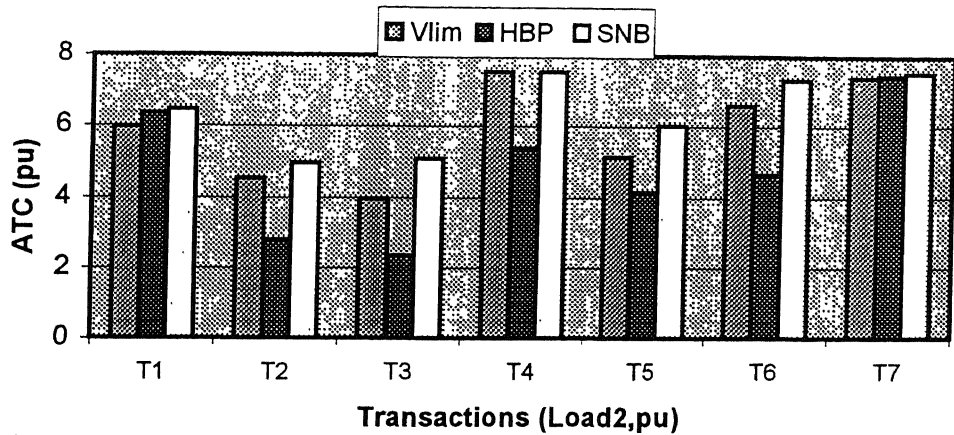
Fig. 3.5 ATC for 9-Bus System with SVC -Load2 Case

3.5.2 39-bus, 10 Generator System

The load bus voltage participation factors corresponding to the critical eigenvalues were computed when Hopf bifurcation (HB) and saddle node bifurcation (SNB) limits were considered for ATC determination. These are listed for the few critical buses in Tables 3.8 and 3.9 respectively for HB and SNB cases.

Table 3.8
Critical Load Bus Voltage Participation Factors for HB Limit -Load1 Case
(39-bus, 10-generator system)

T1		T2		T3		T4		T5	
Bus	PF	Bus	PF	Bus	PF	Bus	PF	Bus	PF
121	0.0190	31	0.0193	31	0.0199	31	0.0195	20	0.0251
15	0.0216	15	0.0221	15	0.0227	15	0.0224	31	0.0285
16	0.0220	16	0.0225	11	0.0230	16	0.0228	19	0.0331
11	0.0229	11	0.0234	16	0.0231	11	0.0233	15	0.0376
17	0.0231	17	0.0238	17	0.0244	17	0.0240	16	0.0388
18	0.0235	18	0.0242	18	0.0247	18	0.0244	17	0.0429
19	0.0257	19	0.0267	19	0.0264	19	0.0263	**18**	**0.0430**

Table 3.9
Critical Load Bus Voltage Participation Factors for SNB Limit - Load1 Case
(39-bus, 10-generator system)

T1		T2		T3		T4		T5	
Bus	PF	Bus	PF	Bus	PF	Bus	PF	Bus	PF
20	0.0251	20	0.0260	20	0.0266	14	0.0276	14	0.0268
31	0.0285	31	0.0299	31	0.0304	31	0.0323	31	0.0311
19	0.0331	19	0.0361	19	0.0344	19	0.0365	19	0.0358
15	0.0376	15	0.0408	15	0.0407	15	0.0462	15	0.0433
16	0.0388	16	0.0420	16	0.0419	16	0.0475	16	0.0445
17	0.0429	17	0.0475	17	0.0471	17	0.0550	17	0.0508
18	**0.0430**	**18**	**0.0479**	**18**	**0.0473**	**18**	**0.0553**	**18**	**0.0511**

It is observed that bus 18 has the maximum participation in the critical mode corresponding to saddle node bifurcation for all the cases. However, at Hopf bifurcation, bus 19 has maximum participation factor in all transactions except one transaction for which bus 18 has the maximum participation factor. Since, bus 18 has maximum participation factor in most of the cases, it was selected for the placement of SVC. Further simulations revealed that SVC at bus 18 is more effective in enhancing the ATC as compared to that when it is placed at bus 19.

The ATCs for the different transactions 'T1'–'T5' defined in chapter-2 corresponding to 'Load1' case have been presented in Tables 3.10 and 3.11 corresponding to HB and SNB limits respectively. Tables 3.12 and 3.13 give the corresponding results for the 'Load2' case. It is interesting to note for Table 3.10 that Hopf bifurcation gets eliminated in case of transaction T2.

Table 3.10
Dynamic ATC using Hopf Bifurcation Criteria - Load1 Case
(39-bus, 10-Generator System with SVC at bus 18)

Transaction	Load	ATC	Ploss	Qloss	Voltage Profile Critical Buses				
Base Case	5.22	-	0.471	-0.373	V_{32}=0.945	V_{35}=0.958	V_{14}=0.960	V_{34}=0.962	V_{33}=0.965
T1	**14.20**	**8.98**	**0.597**	**6.777**	V_{32}=0.928	V_{14}=0.944	V_{16}=0.945	V_{15}=0.946	V_{17}=0.948
T2	*30.64*	*25.42*	*2.773*	*40.956*	V_{19}=0.786	V_{18}=0.849	V_{17}=0.851	V_{14}=0.866	V_{15}=0.866
T3	17.85	12.63	0.967	14.608	V_{32}=0.886	V_{33}=0.907	V_{31}=0.908	V_{20}=0.908	V_{34}=0.914
T4	**12.32**	**7.10**	**1.171**	**6.614**	V_{32}=0.935	V_{14}=0.944	V_{35}=0.946	V_{34}=0.950	V_{33}=0.954
T5	31.42	26.20	4.038	75.437	V_{13}=0.722	V_{14}=0.749	V_{38}=0.776	V_{12}=0.794	V_{17}=0.795

T2[**] -- Hopf Bifurcation not observed; Results are corresponding to the SNB.

In case of transactions T1 and T4, the bus voltages at HB are above the minimum bus voltage limits and hence HB becomes the corresponding limit for the ATC determination.

Table 3.14 presents the ATC values after placement of SVC at bus 18 for the two loading scenario, when voltage limits are also considered. Comparing the ATC values given in Tables 3.10 to 3.14 with the corresponding cases without SVC in chapter-2, it is observed that ATC values have increased in all the cases. Bus voltage profile has improved when SVC is considered in the system. Figs. 3.6 and 3.7 compare the ATC for HB, SNB and bus voltage limit cases for 'Load1' and 'Load2' scenario, respectively. In most of the cases, Hopf bifurcation limts constrain the ATC value, whereas in quite a few cases voltage limits became the governing criteria.

Table 3.11
Static ATC using Saddle Node Bifurcation Criteria – Load1 Case
(39-bus, 10-Generator System with SVC at bus 18)

Transaction	Load	ATC	Ploss	Qloss	Voltage Profile at Critical Bus				
Base Case	5.22	-	0.471	-0.373	V_{32}=0.945	V_{35}=0.958	V_{14}=0.960	V_{34}=0.962	V_{33}=0.965
T1	25.16	19.94	1.082	35.358	V_{16}=0.832	V_{15}=0.840	V_{32}=0.851	V_{17}=0.851	V_{31}=0.865
T2	30.64	25.42	2.773	40.956	V_{19}=0.786	V_{18}=0.849	V_{17}=0.851	V_{14}=0.866	V_{15}=0.866
T3	25.42	20.20	2.018	47.253	V_{32}=0.730	V_{20}=0.751	V_{31}=0.756	V_{33}=0.757	V_{34}=0.791
T4	28.81	23.59	8.021	75.100	V_{12}=0.763	V_{13}=0.768	V_{25}=0.803	V_{38}=0.804	V_{14}=0.804
T5	31.69	26.47	5.504	102.131	V_{13}=0.612	V_{14}=0.680	V_{12}=0.686	V_{38}=0.692	V_{14}=0.742

Table 3.12
Dynamic ATC using Hopf Bifurcation Criteria – Load2 Case
(39-bus, 10-Generator System with SVC with SVC at bus 18)

Transaction	Load	ATC	Ploss	Qloss	Voltage Profile at Critical Bus				
Base Case	5.22	-	0.471	-0.373	V_{32}=0.945	V_{35}=0.958	V_{14}=0.960	V_{34}=0.962	V_{33}=0.965
T1	14.98	9.76	0.628	8.334	V_{32}=0.916	V_{17}=0.924	V_{16}=0.926	V_{15}=0.926	V_{18}=0.930
T2	27.25	22.03	2.149	30.500	V_{18}=0.816	V_{17}=0.825	V_{19}=0.830	V_{15}=0.850	V_{16}=0.857
T3	18.64	13.42	1.063	17.600	V_{32}=0.860	V_{31}=0.881	V_{33}=0.884	V_{20}=0.884	V_{17}=0.891
T4	**12.74**	**7.52**	**1.242**	**7.497**	**V_{32}=0.927**	**V_{14}=0.935**	**V_{35}=0.942**	**V_{34}=0.943**	**V_{17}=0.943**
T5	28.29	23.07	2.876	52.793	V_{14}=0.781	V_{13}=0.800	V_{17}=0.808	V_{15}=0.810	V_{18}=0.812

51

भारतीय प्रौ... ...न कानपुर
अवाप्ति क्र॰ A...137931

Table 3.13

Static ATC using Saddle Node Bifurcation Criteria – Load2 Case

(39-bus, 10-Generator System with SVC at bus 18)

Transaction	Load	ATC	Ploss	Qloss	Voltage Profile at Critical Bus				
Base Case	5.22	-	0.471	-0.373	V_{32}=0.945	V_{35}=0.958	V_{14}=0.960	V_{34}=0.962	V_{33}=0 96
T1	23.07	17.95	1.020	29.947	V_{16}=0.825	V_{17}=0.827	V_{15}=0.829	V_{18}=0.840	V_{32}=0 84
T2	27.25	22.03	2.149	30.500	V_{18}=0.816	V_{17}=0.825	V_{19}=0.830	V_{15}=0.850	V_{16}=0.85
T3	23.07	17.85	1.634	35.106	V_{32}=0.772	V_{31}=0.795	V_{20}=0.797	V_{33}=0.800	V_{16}=0.82
T4	27.77	22.55	7.012	67.795	V_{13}=0.776	V_{14}=0.782	V_{12}=0.791	V_{17}=0.807	V_{15}=0.80
T5	28.29	23.07	2.876	52.793	V_{14}=0.781	V_{13}=0.799	V_{17}=0.808	V_{15}=0.810	V_{18}=0.81

Table 3.14

ATC Value Determination on the Basis of Voltage Limit Criteria

(39-bus, 10-Generator System with SVC at bus 18)

Transaction	Load1	ATC1	Load2	ATC2
Base Case	5.22	-	5.22	-
T1	20.72	15.50	17.85	12.63
T2	25.94	20.72	20.98	15.76
T3	16.29	11.07	14.72	9.50
T4	20.98	15.76	18.64	13.42
T5	22.03	16.81	19.68	14.45
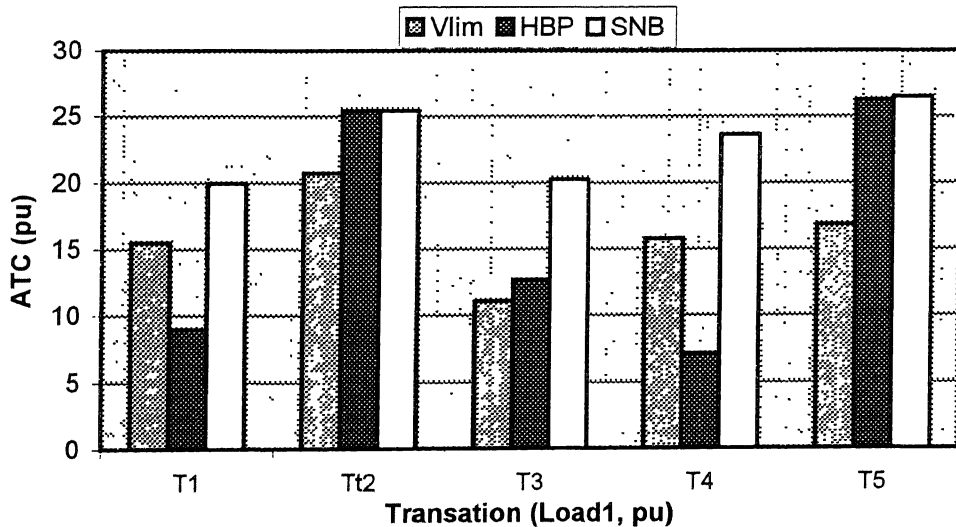
Fig. 3.6 ATC for 39-Bus System with SVC -Load1 Case.
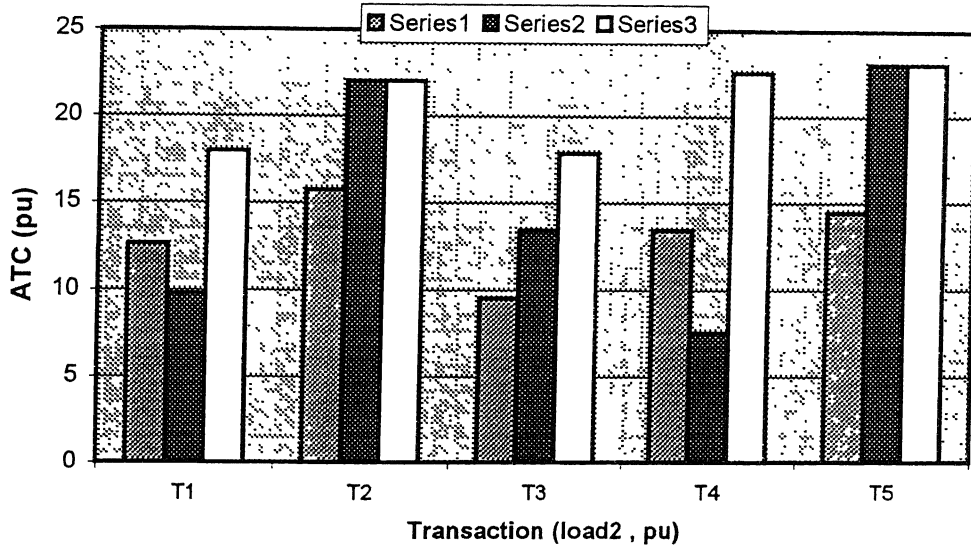
Fig. 3.7 ATC for 39-Bus System with SVC - Load2 Case.

3.5.3 Impact of Change in SVC Regulator Gain

In order to observe the impact of change in voltage regulation slope of SVC on its performance for ATC enhancement, the slope was changed to 5% (K_R=20) from its earlier value of 1% (K_R=100). The results, obtained on 39-bus New England system, are presented in Tables 3.15 & 3.16 for different transaction scenario.

Comparing these results with those in Table 3.10, 3.11 and 3.14, it is observed that static ATC corresponding to SNB and voltage limits have considerably reduced when K_R was reduced to 20% from its original value of 100%. However, the dynamic ATC variation does not show any specific trend.

Table 3.15
Dynamic ATC using Hopf Bifurcation Criteria-Load1 Case
(39-bus, 10-Generator System with SVC at bus 18, K_R=20)

Transaction	Load	ATC	Ploss	Qloss	Voltage Profile at Critical Bus				
Base Case	5.22	-			V_{32}=0.945	V_{35}=0.958	V_{14}=0.960	V_{34}=0.962	V_{33}=0.965
T1	14.46	9.24	0.630	8.117	V_{32}=0.909	V_{17}=0.910	V_{18}=0.913	V_{15}=0.916	V_{16}=0.916
T2	25.42	20.20	1.862	25.595	V_{18}=0.810	V_{17}=0.820	V_{15}=0.848	V_{19}=0.851	V_{16}=0.856
T3	17.85	12.63	1.035	16.733	V_{32}=0.855	V_{17}=0.874	V_{31}=0.876	V_{18}=0.878	V_{33}=0.880
T4	12.74	7.52	1.251	7.772	V_{32}=0.920	V_{14}=0.928	V_{17}=0.930	V_{18}=0.931	V_{15}=0.934
T5	25.16	19.94	2.101	36.576	V_{14}=0.825	V_{17}=0.831	V_{18}=0.832	V_{15}=0.840	V_{32}=0.845

Table 3.16
Static ATC using SNB and Voltage limit Criteria-Load1 Case
(39-bus, 10-Generator System with SVC at bus 18, K_R=20)

Transaction	Load	ATC	Ploss	Qloss	Min. Voltage limit	
Base Case	5.22	-				
T1	22.55	17.33	1.431	46.523	15.76	10.54
T2	27.51	22.29	2.633	40.237	18.90	13.68
T3	22.29	17.07	1.681	36.330	13.41	8.19
T4	28.27	23.05	9.076	95.777	17.59	12.37
T5	28.29	23.07	3.112	58.044	18.37	13.15

Fig. 3.8 shows the ATC Values corresponding to different limits when the regulator gain in the SVC control loop is decreased to 20.
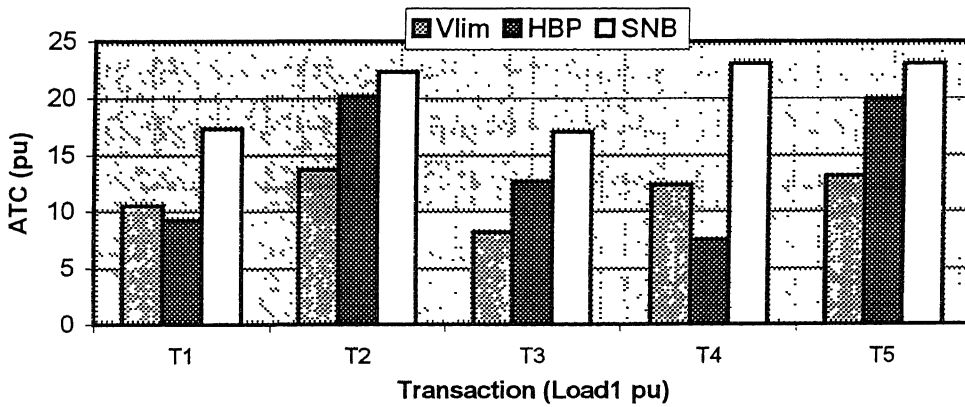
Fig.3.8 ATC for 39-Bus System with SVC (Load1)
(Kr=20)

3.6 Conclusions

In this chapter a method based on state participation factor analysis has been used to determine optimal placement of SVC. SVC placement has been considered only at load buses where voltage state participation to the critical mode corresponding to HB or SNB is maximum. The impact of SVC on ATC enhancement has been studied on 9-bus WSCC and 39-bus New England systems.

The main conclusions of the study are :

1. Placement of SVC at an optimal location (load bus 5 in case of 9-bus system and bus 18 in case of 39-bus system) has enhanced both static and dynamic ATC values for all the transactions in the two loading scenario.

2. With the placement of SVC, Hopf Bifurcation criterion became the binding constraint for ATC in several transactions for both the system limits, e.g. transaction T1, T3 and T4 in 39-bus system 'Load1' case, T2 to T6 in the 9-bus WSCC system 'Load1' case.

3. Voltage criteria are still observed to be limiting constraint in some transactions, specifically in the 39-bus system. However the voltage profile improves with inclusion of SVC in all the cases.

4. With the placement of SVC the Hopf bifurcation gets completely eliminated in few transaction cases e.g. transactions T2 and T5 in the 39-bus system 'Load2' case.

5. Reduction in the gain setting, K_R, or increase in the voltage regulation slope of the SVC has reduced static ATC with respect to SNB limit and voltage limits in all the cases. However, the dynamic ATC has increased in few cases.

CHAPTER 4

CONCLUSIONS

Most of the power utilities worldwide are undergoing restructuring in order to encourage competition at generation and distribution levels. Unlike in the conventional monopolistic electric utilities, market forces guide the generation schedule and load dispatch in deregulated market. This may result in very different loading patterns than those expected in a conventional integrated structure. The Independent System Operator (ISO) is primarily responsible for the Grid operation and has to honour all the contracts committed on the basis of ATC posted on the Open Access Same-time Information System (OASIS). The precise determination of the value of ATC becomes very crucial for secure operation of the system. If it is under-estimated the market will be unduly stressed and it will jeopardize the market spirit while the system capabilities remain unutilized. On the other hand, if it is over-estimated the system security is threatened and the ISO may have to curtail some of the transactions for which it will incur a loss of revenue. Therefore, the ISO should make an exhaustive study of the system and all its constraints while assessing the value of ATC.

This thesis has made an attempt to apply bifurcation concept for the determination of ATC. The limits imposed by occurrence of Hopf bifurcation (HB) and saddle node (SNB) bifurcation has been included to determine dynamic ATC and static ATC values, respectively. In addition, the bus voltage limits have also been considered for the ATC determination. A method based on eigenvalue analysis and participation factors has been utilized to identify critical load bus for optimal placement of SVC. The impact of SVC on ATC enhancement has also been studied. The ATC determination with and without SVC has been carried out for two different loading scenario 'Load1' case (when only real power has been increased) and 'Load2' case (when both real and reactive power has been increased) on WSCC 9-bus and New England 39-bus systems.

The main findings of the studies carried out in the thesis are as follows :

1. Hopf bifurcation occurs before saddle node bifurcation in most of the transactions studied. Hence the dynamic ATC corresponding to Hopf bifurcation is found to be

56

less than that corresponding to static ATC at saddle node bifurcation. However, only in few cases Hopf bifurcation did not occur till the saddle node bifurcation.

2. Voltage limit criterion is found to be the limiting constraint in most of the transactions without SVC. With increased system loading, voltage decline is observed - the decline being more rapid at higher loadings when the reactive power transmission losses increase.

3. When reactive power demand was also increased along with the real power demand ('Load2' case at constant power factor) the ATC values drastically reduced as compared to the 'Load1' case when only the real power demand was increased. Also, it adversely affected the system voltage profile. Hence for ATC calculation, both real and reactive power change in loadings must be considered.

4. The voltage dependent 'ZIP' load model resulted in different values of ATC as compared to the constant power model in most of the cases. This reveals the sensitivity of ATC upon the load modelling and hence, the importance of using a realistic load model.

5. Application of SVC at the load bus having maximum participation for voltage state to the critical mode at the Hopf bifurcation and saddle node bifurcation is found to enhance the ATC value in all the cases. System voltage profile got improved after placement of the SVC. This highlights the importance of reactive power management as an inseparable ancillary service in the restructured electricity market.

6. With the improved system voltage profile after placement of SVC, Hopf bifurcation criterion was found to be the limiting constraint in several cases. Hopf bifurcation mainly depends upon the dynamics of state variables at the equilibrium point. Thus dynamic ATC determination is important as it may restrict the power transaction in most of the cases.

7. SVC has little effect on minimizing the real power losses in the system. Though there is marginal decrease in the real power loss for the same loading level, the losses are very high at the limiting ATC loadings. Also, the requirement of reactive power loading increases sharply after a certain limit.

8. The voltage regulation slope value of SVC output characteristic has a pronounced effect on ATC values. As the slope is increased, the system voltage profile deteriorates and the ATC values for the different transactions decrease. This trend was obsevedin the static ATC values. However, the dynamic ATC value did not show any specific trend for the change in SVC voltage regulation slope.

During the course of the research work carried out in this thesis, the following areas of further research were identified for effective computation of ATC :

➤ In the present work, loads and generations have been increased in a predefined direction for computation of ATC. This may not lead to the closest point of Hopf or saddle node bifurcation. Computation and analysis of the minimum value of dynamic and static ATC on the basis of Hopf bifurcation and saddle node bifurcations closest to the operating point would enable the operator to know the worst case margins in the system. More research and study is required for developing such a methodology to calculate these quantities within a reasonable time frame.

➤ FACTS controllers are expected to enhance the ATC of the Such an enhancement of ATC by FACTS application can be a promising solution in congestion management but it needs more studies to identify the effectiveness of the various controller (only SVC is considered in the present study) vis-à-vis its cost and contribution to the market.

➤ Research is needed to define a generalized but realistic load model, which incorporates its dynamics, so that the load dynamics can be incorporated in the assessment of dynamic and static ATC values.

REFERENCES

[1]   L. Phillipson and H. L. Willis, *Understanding Electric Utilities and Deregulation*, Marcell Dekker Inc., New York, 1999.

[2]   N. G. Hingorani and L. Gyugyi, *Understanding FACTS Concepts and Technology of Flexible AC Transmission Systems*, IEEE Press, New York, 1999.

[3]   Marija Ilic, F. Galiana and L. Fink, *Power System Restructuring*, Kluwer Academic Publishers, USA, 1998.

[4]   P. W. Sauer and M. A. Pai, *Power System Dynamics and Stability*, Prentice-Hall Inc., New Jersey, 1998.

[5]   T. V. Cutsem and C. Vournas, *Voltage Stability of Electric Power Systems*, Kluwer Academic Publishers, USA, 1998.

[6]   K.R. Padiyar, *Power System Dynamics Stability and Control*, John Wiley & Sons (Asia) Pte Ltd., 1996.

[7]   P. Kundur, *Power System Stability and Control*, Mc Graw-Hill Inc., NY, 1994.

[8]   T. J. E. Miller, '*Reactive Power Control in Electrical Systems*, John Wiley & Sons, USA, 1982.

[9]   North American Electric Reliability Council (NERC), "Available Transfer Capability Definitions and Determination", NERC Report, June 1996.

[10] *"Voltage Stability Assessment, Procedures and Guides,"* IEEE/PES Power System Stability Subcommittee Special Publication, Final Draft, January 2001.

      Available at: http://www.power.waterloo.ca.

[11] G. Sombuttwilailert and B. Eua-Arporn, "Iterative Linear Estimation for Total Transfer Capability Evaluation", IEEE Summer Meeting- Vancouver, Jul. 2001.

[12] A. Srivastava, "Determination of the Available Transfer Capability in a Deregulated Power System", *M. Tech. Thesis*, IIT-Kanpur, Mar. 2001.

[13] K. S. Verma and S. N. Singh and H. O. Gupta, "FACTS Devices Location for Enhancement of Total Transfer Capability", IEEE Winter Meeting, Ohio, USA, Jan28-Feb1, 2001, Vol 2, pp 522-527.

[14] Y. Ou and Ch. Singh, "Improvement of Total Transfer Capability Using TCSC and SVC", IEEE PES Winter Meeting, Jan 28- Feb 1, 2001.

[15] G. C. Ejebe, J. G. Waight, M. Santos-Nieto and W. F. Tinney, "Fast Calculation of Linear Available Transfer Capability", *IEEE Trans on Power Systems*, Vol. 15, No. 3, Aug. 2000, pp. 1112-1116.

[16] G. Hamoud, "Assessment of Available Transfer Capability of Transmission Systems", *IEEE Trans on Power Systems*, Vol. 15, No. 1, Feb. 2000, pp. 27-32.

[17] C. P. Gupta, "Voltage Stability Margin Enhancement Using FACTS Controllers", *PhD- Thesis*, IIT-Kanpur, Oct. 2000.

[18] E. D. Tuglie, M. Dicorato, M. L. Scala and P. Scarpellini, "A static Optimization Approach to Assess Dynamic Available Transfer Capibilty", *IEEE Trans on Power Systems*, Vol. 15, No. 3, Aug. 2000, pp. 1069-1076.

[19] M. Shaaban, Y. Ni and F. Wu, "Total Transfer Capability Evaluation for Competitive Power Markets", International Conference on Electric Utility Deregulation and Restructuring and Power Technologies, London, 4-7 April, 2000, npp 114-118.

[20] R. D. Christie, B. F. Wollenberg and I. Wangensteen, "Transmission Management in the Deregulated Environment", *Proceedings of The IEEE*, Vol. 88, No. 2, Feb 2000, pp 170-195.

[21] W. D. Rosehart and C. A. Canizares, "Bifurcation Analysis of Various Power System Models", *Electrical Power and Energy Systems* 21, 1999, pp 171-182.

[22] M. H. Gravener and C. Nwankpa, "Available Transfer Capability and First Order Sensitivity", *IEEE Trans on Power Systems*, Vol. 14, No. 2, May 1999, pp. 512-518.

[23] R. Wang, R. H. Lasseter, J. Meng and F. L. Alvarado, "Fast Determination of Simulataneous Available Transfer Capability (ATC)", PSERC Publications 1999. Available at http://www.pserc.wisc.edu.

[24] G. C. Ejebe, J. Tong, G. G. Waight, J. G. Frame, X. Wang and W. F. Tinney, "Available Transfer Capability Calculations", *IEEE Trans. on Power Systems*, Vol. 13, No. 4, pp 1521-1527, Nov. 1998.

[25] C. A. Cañizares, A. Berizzi, P. Marannino, "FACTS Controllers to Maximize Available Transfer Capability", *Proceedings of Bulk Power Systems Dynamics and Control IV Seminar,* IREP/NTUA, Santorini, Greece, Aug.1998, pp 633-641.

[26] I. A. Hiskens, M. A. Pai and P. W. Sauer, "An Iterative Approach to Calculating Dynamic ATC", *Proceedings of Bulk Power System Dynamics and Control IV - Restructuring*, Santorini, Greece, Aug. 1998.

[27] K. N. Srivastava, "Investigations Into Static and Dynamic Aspects of Voltage Stability", *PhD Thesis*, IIT-Kanpur, Dec.-1994.

[28] "Static Var Compensator Models for Power Flow and Dynamic Performance Simulation", IEEE Special Stability Controls Working Group, *IEEE Transaction on Power Systems*, Vol. 9, No. 1, Feb. 1994.

[29] V. Ajjarappu and C. Christy, "The Continuation Power Flow: A Tool for Steady State Voltage Stability Analysis", *IEEE Trans on Power Systems*, Vol. 7, No. 1,Feb. 1992, pp. 416-423.

[30] P. W. Sauer and M. A. Pai, "Power System Steady State Stability and the Load Flow Jacobian", *IEEE Trans. on Power Systems*, Vol. 5, No. 4, Nov. 1990, pp. 1374-1382

APPENDIX A
WSSC 3-machine, 9-bus System
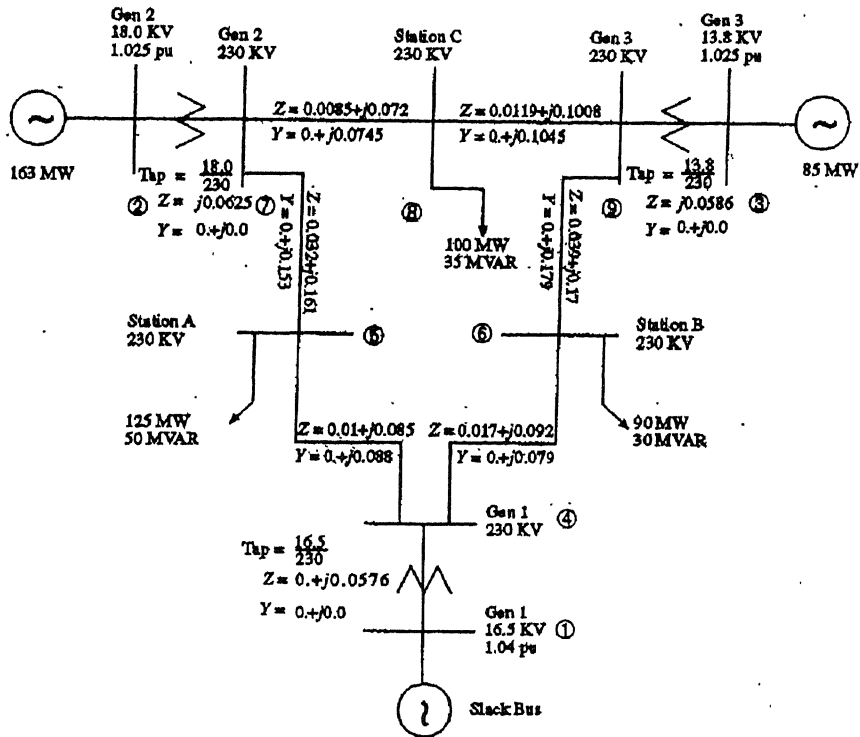
Fig. A-1 One Line Diagram of WSCC 9-bus System.

Base Case Load Flow Results

Bus	Voltage	phase(deg)	Pgen	Qgen	Pload	Qload
1	1.040	0.00	0.7164	0.2705	0.0000	0.0000
2	1.025	9.28	1.6300	0.0665	0.0000	0.0000
3	1.025	4.66	0.8500	-0.1086	0.0000	0.0000
4	1.026	-2.22	-0.0000	0.0000	0.0000	0.0000
5	0.996	-3.99	-0.0000	0.0000	1.2500	0.5000
6	1.013	-3.69	-0.0000	0.0000	0.9000	0.3000
7	1.026	3.72	0.0000	0.0000	0.0000	0.0000
8	1.016	0.73	-0.0000	0.0000	1.0000	0.3500
9	1.032	1.97	0.0000	0.0000	0.0000	0.0000

Line & Transformer Data

	From	To	R_line	X_line	Y_charging	Tapping
Transformers:						
	4	1	0.0000	0.0576	0.0000	1
	7	2	0.0000	0.0625	0.0000	1
	9	3	0.0000	0.0586	0.0000	1
Lines:						
	4	6	0.0170	0.0920	0.1580	
	4	5	0.0100	0.0850	0.1760	
	5	7	0.0320	0.1610	0.3060	
	6	9	0.0390	0.1700	0.3580	
	7	8	0.0085	0.0720	0.1490	
	8	9	0.0119	0.1008	0.2090	

Machine Data

Gen	H	X_d	X_d'	X_q	X_q'	T_{do}'	T_{qo}'
1	23.6	0.1460	0.0608	0.0969	0.0969	8.96	0.31
2	6.4	0.8958	0.1198	0.8645	0.1969	6.00	0.54
3	3.0	1.3125	0.1813	1.2578	0.2500	5.89	0.60

Exciter Data

The same exciter is used in all the three generators. The exciter data are given below :

K_A = 20.0
T_A = 0.2 (sec)
K_E = 1.0
T_E = 0.314
K_F = 0.063
T_F = 0.35

The satutration function of the exciter is

$$S_{Ei}(E_{fdi}) = 0.0039e^{1.555 E_{fdi}} \quad \text{for i=1,2,3 (all generators).}$$

39-bus, 10-generator New England System
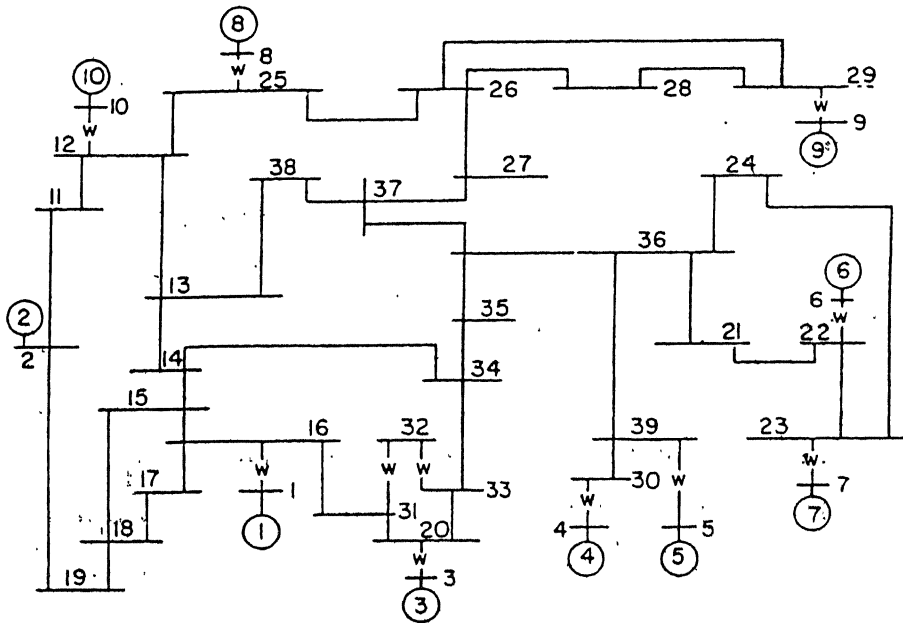
Fig. B-1 One line diagram of New England 39-bus System.

Base Case Load-flow Results

Bus	Voltage	phase(deg)	Pgen	Qgen	Pload	Qload
1	0.980	0.00	5.527	1.687	0.092	0.046
2	1.030	−11.06	10.000	2.425	11.040	2.500
3	0.980	2.36	6.500	1.705	0.000	0.000
4	1.010	3.22	5.080	1.673	0.000	0.000
5	0.990	4.30	6.320	0.760	0.000	0.000
6	1.040	5.35	6.500	2.669	0.000	0.000
7	1.060	8.13	5.600	2.415	0.000	0.000
8	1.020	1.95	5.400	0.239	0.000	0.000
9	1.020	7.71	8.300	0.631	0.000	0.000
10	1.040	−4.01	2.500	1.767	0.000	0.000
11	1.033	−9.40	−0.000	0.000	0.000	0.000
12	1.010	−6.48	0.000	0.000	0.000	0.000
13	0.979	−9.51	0.000	0.000	3.220	0.024
14	0.945	−10.45	0.000	0.000	5.000	1.840
15	0.947	−9.19	−0.000	0.000	0.000	0.000
16	0.948	−8.41	−0.000	0.000	0.000	0.000
17	0.940	−10.88	0.000	0.000	2.338	0.840
18	0.941	−11.45	0.000	0.000	5.220	1.760
19	1.006	−11.27	0.000	0.000	0.000	0.000

20	0.954	-5.63	0.000	0.000	0.000	0.000
21	0.978	-4.34	0.000	0.000	2.740	1.150
22	1.007	0.26	-0.000	0.000	0.000	0.000
23	1.006	-0.02	-0.000	0.000	2.745	0.840
24	0.967	-6.83	0.000	0.000	3.086	0.922
25	1.019	-4.97	-0.000	0.000	2.240	0.472
26	1.005	-6.23	-0.000	0.000	1.390	0.170
27	0.985	-8.38	0.000	0.000	2.810	0.755
28	1.009	-2.43	0.000	0.000	2.060	0.276
29	1.012	0.53	0.000	0.000	2.835	0.269
30	0.980	-1.99	0.000	0.000	6.280	1.030
31	0.951	-6.57	-0.000	0.000	0.000	0.000
32	0.931	-6.56	0.000	0.000	0.075	0.880
33	0.952	-6.42	-0.000	0.000	0.000	0.000
34	0.950	-8.27	-0.000	0.000	0.000	0.000
35	0.951	-8.59	0.000	0.000	3.200	1.530
36	0.967	-6.93	0.000	0.000	3.294	0.323
37	0.975	-8.15	-0.000	0.000	0.000	0.000
38	0.975	-9.15	0.000	0.000	1.580	0.300
39	0.979	-0.98	0.000	0.000	0.000	0.000

Line & Transformer Data

From	To	R_line	X_line	Y_charging	Tapping
Transformer:					
39	30	0.0007	0.0138	0.0000	1
39	5	0.0007	0.0142	0.0000	1
32	33	0.0016	0.0435	0.0000	1
32	31	0.0016	0.0435	0.0000	1
30	4	0.0009	0.0180	0.0000	1
29	9	0.0008	0.0156	0.0000	1
25	8	0.0006	0.0232	0.0000	1
23	7	0.0005	0.0272	0.0000	1
22	6	0.0000	0.0143	0.0000	1
20	3	0.0000	0.0200	0.0000	1
16	1	0.0000	0.0250	0.0000	1
12	10	0.0000	0.0181	0.0000	1
Line Data:					
37	27	0.0013	0.0173	0.3216	
37	38	0.0007	0.0082	0.1319	
36	24	0.0003	0.0059	0.0680	
36	21	0.0008	0.0135	0.2548	
36	39	0.0016	0.0195	0.3040	
36	37	0.0007	0.0089	0.1342	
35	36	0.0009	0.0094	0.1710	
34	35	0.0018	0.0217	0.3660	
33	34	0.0009	0.0101	0.1723	
28	29	0.0014	0.0151	0.2490	
26	29	0.0057	0.0625	1.0290	
26	28	0.0043	0.0474	0.7802	
26	27	0.0014	0.0147	0.2396	
25	26	0.0032	0.0323	0.5130	
23	24	0.0022	0.0350	0.3610	

22	23	0.0006	0.0096	0.1846
21	22	0.0008	0.0135	0.2548
20	33	0.0004	0.0043	0.0729
20	31	0.0004	0.0043	0.0729
19	2	0.0010	0.0250	1.2000
18	19	0.0023	0.0363	0.3804
17	18	0.0004	0.0046	0.0780
16	31	0.0007	0.0082	0.1389
16	17	0.0006	0.0092	0.1130
15	18	0.0008	0.0112	0.1476
15	16	0.0002	0.0026	0.0434
14	34	0.0008	0.0129	0.1382
14	15	0.0008	0.0128	0.1342
13	38	0.0011	0.0133	0.2138
13	14	0.0013	0.0213	0.2214
12	25	0.0070	0.0086	0.1460
12	13	0.0013	0.0151	0.2572
11	12	0.0035	0.0411	0.6987
11	2	0.0010	0.0250	0.7500

The line-charging admittance data given above is taken as full-line charging.

Machine Data

Gen	H	X_d	X_d'	X_q	X_q'	T_{do}'	T_{qo}'
1	30.3	0.2950	0.0647	0.2820	0.0647	6.56	1.50
2	500.0	0.0200	0.0060	0.0190	0.0060	6.00	0.70
3	35.8	0.2495	0.0531	0.2370	0.0531	5.70	1.50
4	26.0	0.3300	0.0660	0.3100	0.0660	5.40	0.44
5	28.6	0.2620	0.0436	0.2580	0.0436	5.69	1.50
6	34.8	0.2540	0.0500	0.2410	0.0500	7.30	0.40
7	26.4	0.2950	0.0490	0.2920	0.0490	5.66	1.50
8	24.3	0.2900	0.0570	0.2800	0.0570	6.70	0.41
9	34.5	0.2106	0.0570	0.2050	0.0570	4.79	1.96
10	42.0	0.2000	0.0040	0.1960	0.0040	5.70	0.05

For All Machines Ra=0.

AVR data-

K_A=25 , T_A=0.025.

D/M ratio = 0.1 for each machine.